JP0150752

JAERI-Tech
2001-054

VARIATION OF RADIOLOGICAL CONSEQUENCES UNDER VARIOUS WEATHER CONDITIONS

August 2001

Xinhe LIU and Toshimitsu HOMMA

日本原子力研究所
Japan Atomic Energy Research Institute

編集兼発行　日本原子力研究所

Variation of Radiological Consequences under Various Weather Conditions

Xinhe LIU* and Toshimitsu HOMMA

Department of Reactor Safety Research
Nuclear Safety Research Center
Tokai Research Establishment
Japan Atomic Energy Research Institute
Tokai-mura, Naka-gun, Ibaraki-ken

(Received July 2, 2001)

Stratified sampling method of determining weather sequences is widely used in Probabilistic Safety Assessment Level-3 calculations with an intention to predict the complete spectrum of the accident consequences. Intensive calculations were performed for every weather bin in order to get a general view of consequence variation in response to the indices used in the weather bin categorization procedures. The results of this case study demonstrated that there must be important factors, such as time-integrals of meteorological parameters other than initial weather conditions, which might influence the consequences for a given accident. Further improvement is needed for the choice of criteria for grouping weather sequences in the stratified sampling scheme.

Keywords: Probabilistic Safety Assessment, Accident Consequence Assessment, Meteorological Sampling scheme, Stratified Sampling

*LIU Xinhe was a visiting researcher from China Institute of Atomic Energy under the auspices of the Science and Technology Agency Scientist Exchange Program.

JAERI-Tech 2001-054

様々な気象条件による放射線影響の変化

日本原子力研究所東海研究所安全性試験研究センター原子炉安全工学部
劉　新河※・本間　俊充

（2001年7月2日受理）

確率論的安全評価のレベル3計算においては、事故影響の完全なスペクトラムを予測するために気象シーケンスを決めるための層別サンプリング法が広く用いられている。気象ビン分類で用いる指標に対応した事故影響の変化の一般的な知見を得るために、様々な気象ビンに対する広範な計算を行った。この研究の結果から、放出時最初の気象条件の他に、例えば気象パラメータの時間積分のような事故影響結果に影響を与える因子があることが示唆された。層別サンプリング法における気象シーケンスのグループ化規準の選定には改善の余地がある。

※劉新河は、科学技術庁原子力研究研究交流制度で来日した中国原子能科学研究院からの客員研究員である。
東海研究所：〒319-1195　茨城県那珂郡東海村白方白根2-4

Contents

目　次

1. INTRODUCTION

Probabilistic Safety Assessment was developed in the United Kingdom in 1960s for nuclear power plant siting [1]. The first comprehensive application of PSA of postulated nuclear accidents dates back to the Reactor Safety Study in 1975 [2]. The CRAC computer code was developed as one part of this landmark study. Since then PSAs have become widely utilized for the safety assessment of nuclear facilities and PSA computer codes have been developed quite extensively [3]. For example, a number of modified versions of CRAC have been developed in US, and the first version of the MACCS code was developed by the Sandia National Laboratories in 1983 [4]. In Europe, the program UFOMOD was developed in 1979 by Kernforschungszentrum Karlsruhe [5], MARC developed by UK National Radiological Protection Board (NRPB) in 1981 [6], CONDOR jointly developed by AEA Technology, Berkeley Technology Center of Nuclear Electric and UK NRPB in 1993 [7], the COSYMA system developed in the Commission of the European Communities during the late 1980's [8]. In Japan, the program OSCAAR was developed by the Japan Atomic Energy Research Institute [9]. These PSA codes are capable of depicting the full spectrum of the consequences resulting from major nuclear accidents, by calculating the probabilities of events with potential public health consequences and the magnitudes of these potential health consequences as well. Therefore, PSA has been recognized as a systematic process and an important methodology in the design and operation of nuclear power plants [10].

PSAs aim at the full distribution of major nuclear accident consequences, by computing the probabilities of events with potential public health consequences and the magnitude of these potential consequences. Ideally, calculations of atmospheric dispersion, food-chain transfer, dose and health effects estimation should be conducted for every possible sequence of weather conditions. Computer resources are not sufficient to accomplish this formidable task, and a representative selection of weather sequences has to be utilized instead. The selection should be made in such a way that the sequences chosen represent the complete range of all the possible sequences and yield the full spectrum of the consequences of nuclear accidents.

The selection of weather sequences is the selection of starting time of sequences in a meteorological data file. Two simple methods are random sampling and cyclic sampling. It is obvious that these sampling schemes tend to collect the more common sequences frequently and overlook the rare ones that can lead to most severe consequences. If such a rare sequence were sampled, the probability distribution would be distorted. A more sophisticated method is stratified sampling. The intentions of it are to sort the weather sequences leading to comparable consequences into groups or bins and then to provide a realistic representation of complete range of the weather sequences without overlooking those kind of sequences that can be instrumental in producing major consequence impacts [11].

Categorization of weather sequences is of critical importance in the stratified sampling methods. There are different schemes for categorizing weather sequences [12]. Recent experiences of running MACCS and COSYMA, two of the most well-known PSA codes, demonstrated that cyclic sampling seemed to present results better than stratified sampling in the case studies [13, 14]. These results suggest that further work on meteorological sampling would be justified [15].

The objective of this work is to investigate the divergence of the consequences in each bin and the variation of consequences for different bins. It is expected to get some insight for the modification of stratified sampling methods with the extensive calculations and preliminary analysis of the results.

2. CALCULATION CONDITIONS

2.1 Initial assessment of the meteorological data

As is one part of this study, a simple FORTRAN program METBIN was developed for weather sequence categorization to be performed exactly based upon the description of weather bin and the correspondent algorithm in the model description of MACCS system [11]. METBIN was used as an auxiliary tool to group the weather sequences in this study. Table 1 shows the weather bin description used in this study.

METBIN grouped the full set of hourly weather data into two types: Wet and Dry. Dry sequences were then divided into 16 bins based on their initial atmospheric stability class and initial wind speed. Stability classes A and B were treated identically, and so were stability classes C and D. As shown in Table 1, the numbers of initial wind speed break points were one, five, three and three for stability classes A/B, C/D, E and F, respectively.

Categorization of Wet sequences was based on the intensity of the first rainfall and the spatial interval in which the plume segment ran into the first rainfall. As described in [4], endpoints of the rain distance interval were 3.22, 5.63, 11.27, 20.92, 32.19 km, respectively, the three rain intensity breakpoints were set at 2, 4, 6 mm/hr, respectively. Therefore, wet sequences were classified into 20 bins.

Eventually, a list of starting times of the weather sequences was obtained for each bin when METBIN was operated with the meteorological data file provided by the MACCS system.

Table 1. Weather bin description in the stratified sampling

Bin Number	Bin Notation	Description of Weather Sequences in the Bin
B01	B 3	Initial stability classes A and B, with initial wind speed ≦ 3 m/s.
B02	B 4	Initial stability classes A and B, with initial wind speed > 3 m/s.
B03	D 1	Initial stability classes C and D, with initial wind speed ≦ 1 m/s.
B04	D 2	Initial stability classes C and D, with initial wind speed > 1 and ≦ 2 m/s.
B05	D 3	Initial stability classes C and D, with initial wind speed > 2 and ≦ 3 m/s.
B06	D 4	Initial stability classes C and D, with initial wind speed > 3 and ≦ 5 m/s.
B07	D 5	Initial stability classes C and D, with initial wind speed > 5 and ≦ 7 m/s.
B08	D 6	Initial stability classes C and D, with initial wind speed > 7 m/s.
B09	E 1	Initial stability class E, with initial wind speed ≦ 1 m/s.
B10	E 2	Initial stability class E, with initial wind speed > 1 and ≦ 2 m/s.
B11	E 3	Initial stability class E, with initial wind speed > 2 and ≦ 3 m/s.
B12	E 4	Initial stability class E, with initial wind speed > 3 m/s.
B13	F 1	Initial stability class F, with initial wind speed ≦ 1 m/s.
B14	F 2	Initial stability class F, with initial wind speed > 1 and ≦ 2 m/s.
B15	F 3	Initial stability class F, with initial wind speed > 2 and ≦ 3 m/s.
B16	F 4	Initial stability class F, with initial wind speed > 3 m/s.
B17	R1 3	First occurrence of rainfall of intensity ≦ 2 mm/hr in the interval ≦ 3.22 km
B18	R1 6	First occurrence of rainfall of intensity ≦ 2 mm/hr in the interval > 3.22 and ≦ 5.63 km
B19	R1 11	First occurrence of rainfall of intensity ≦ 2 mm/hr in the interval > 5.63 and ≦ 11.27 km
B20	R1 21	First occurrence of rainfall of intensity ≦ 2 mm/hr in the interval > 11.27 and ≦ 20.92 km

B21	R1	32	First occurrence of rainfall of intensity ≦ 2 mm/hr in the interval > 20.92 and ≦ 32.19 km
B22	R2	3	First occurrence of rainfall of intensity > 2 and ≦ 4 mm/hr in the interval ≦ 3.22 km
B23	R2	6	First occurrence of rainfall of intensity > 2 and ≦ 4 mm/hr in the interval > 3.22 and ≦ 5.63 km
B24	R2	11	First occurrence of rainfall of intensity > 2 and ≦ 4 mm/hr in the interval > 5.63 and ≦ 11.27 km
B25	R2	21	First occurrence of rainfall of intensity > 2 and ≦ 4 mm/hr in the interval > 11.27 and ≦ 20.92 km
B26	R2	32	First occurrence of rainfall of intensity > 2 and ≦ 4 mm/hr in the interval > 20.92 and ≦ 32.19 km
B27	R3	3	First occurrence of rainfall of intensity > 4 and ≦ 6 mm/hr in the interval ≦ 3.22 km
B28	R3	6	First occurrence of rainfall of intensity > 4 and ≦ 6 mm/hr in the interval > 3.22 and ≦ 5.63 km
B29	R3	11	First occurrence of rainfall of intensity > 4 and ≦ 6 mm/hr in the interval > 5.63 and ≦ 11.27 km
B30	R3	21	First occurrence of rainfall of intensity > 4 and ≦ 6 mm/hr in the interval > 11.27 and ≦ 20.92 km
B31	R3	32	First occurrence of rainfall of intensity > 4 and ≦ 6 mm/hr in the interval > 20.92 and ≦ 32.19 km
B32	R4	3	First occurrence of rainfall of intensity > 6 mm/hr in the interval ≦ 3.22 km
B33	R4	6	First occurrence of rainfall of intensity > 6 mm/hr in the interval > 3.22 and ≦ 5.63 km
B34	R4	11	First occurrence of rainfall of intensity > 6 mm/hr in the interval > 5.63 and ≦ 11.27 km
B35	R4	21	First occurrence of rainfall of intensity > 6 mm/hr in the interval > 11.27 and ≦ 20.92 km
B36	R4	32	First occurrence of rainfall of intensity > 6 mm/hr in the interval > 20.92 and ≦ 32.19 km

2.2 Modification and operation of the MACCS code

Version 1.5.11.1 of MACCS was used for this study after it was modified in the environment of DIGITAL VISUAL FORTRAN. The modifications were mainly limited in I/O statements and some SAVE statements. An alteration of an operand was made in one IF statement for the classification of weather sequences in order to keep complete consistence with the model description in [4] and [10]. After its successful implementation in the Digital Visual Fortran environment, the MACCS code was run massively using a batch file.

Because some bins have a large number of sequences, it would be impractical and unnecessary to make a trial for every sequence. Trial numbers were determined for the weather bin in such a way that the calculation results could be representative of the ranges of the consequences in the bins and total number of trials be kept as small as possible. 100 sequences were seasonally sampled from the major bins that had several hundreds of members. All the sequences were sampled from the minor bins that had about or less than 100 hundreds members. About 900 hundreds of trials were conducted. The calculation results were transferred to Microsoft Excel for further analysis.

2.3 Preparation of the input files

The source term data, geographic data and meteorological data provided with the distribution of the MACCS code was utilized in this study. The meteorological data and site data files were used for the Surry plant in US. The main characteristics of the source terms were given in Table 2. The choice of atmospheric dispersion model was wind-shift without rotation. Hence each plume segment in the release traveled in the direction that the wind was blowing at the time that its representative time point leaves the reactor, no rotation of shift pattern was performed, and each weather trial yielded one set of results. This choice is believed to produce a more realistic estimation of the consequences.

Table 2. Characteristics of the source terms used

Item	Value
Time before release	3700 sec
Duration of release	1800 sec
Warning time	1300 sec
Release height	0 m
Energy content of release	3.7 MW
Reference inventory	2440 MW(th)

Chemical group	Xe	I	Cs	Te	Sr	Ru	La	Ce	Ba
Release fractions	1.0	0.68	0.64	0.17	0.0042	0.0023	0.00016	0.0004	0.0063

The input files were prepared for each trial by replacing related starting date and hour.

3. RESULTS AND DISCUSSIONS

3.1 Weather bin classification

The calculations for this study consist of two steps. Firstly, initial assessment of the meteorological data was carried out using the METBIN program, weather bin number being assigned to each starting time. Secondly, the MACSS code was run after the input files were prepared.

The weather sequences were categorized into 36 bins. The number of sequences in the bins are given in Table 3.

Table 3. Weather bin classification results calculated using the example meteorological data of MACCS.

Weather Bin	01	02	03	04	05	06	07	08	09
Number of sequences	957	946	86	572	544	658	145	11	148
Weather Bin	10	11	12	13	14	15	18	17	18
Number of sequences	668	758	599	774	759	145	12	352	41
Weather Bin	19	20	21	22	23	24	25	26	27
Number of sequences	103	132	127	74	3	16	24	27	17
Weather Bin	28	29	30	31	32	33	34	35	36
Number of sequences	0	3	5	7	19	1	5	14	8

It can be seen, for the conditions studied, that the number of sequences is distributed quite unevenly. Some bins such as Bin01, Bin02 and Bin13 have sequences more than seven hundreds, while others such as Bin23, Bin28 and Bin33 only have a few sequences or even null. The major 9 bins sum to 6476 sequences, about 74% of the total number. However, the minor 9 bins sum to 32 sequences, about 0.37% of the total. Provided the sequences yield diverse consequences, the sharp changes of sequence number from bin to bin might be a cause of uncertainty if an identical number of sequences were to be sampled from every bin.

3.2 Consequence calculations

Consequence calculations were performed for every weather bin. Three important indicators of radiological consequences resulting from major nuclear accidents were considered in this study:

(1) Early fatality within 1601 km (EF1k);
(2) Latent cancer mortality within 16 km (LC10);
(3) Latent cancer mortality within 1601 km (LC1k).

The calculation results for every bin are given in Figure 1 through Figure 24.

3.2.1 Dry weather bins

(1) Bin01 and Bin02

Bin01 and Bin02 are composed of weather sequences with atmospheric stability class being A or B. It is shown in Figure 1 that EF1k estimation results of Bin01 vary from 0 to 20 cases, LC10 estimation results spread about two orders of magnitude, LC1k within a factor of about 40. Bin02 has similar results as shown in Figure 1. It can be seen by comparing Figure 1 and Figure 2 that the number of non-zero early fatality decreases remarkably when initial wind speed increases under stability classes A and B.

(2) Bin03 through Bin08

These Bins consist of weather sequences of which the initial atmospheric stability class is C or D. The initial wind speed increases of the bin as the bin number upgrades.

As shown in Figures 3 through 8, the span of EF1k becomes several hundreds cases; LC10 scatters in the range of 10 to 6000 cases; and LC1k changes dramatically from sequences to sequence, covering three orders of magnitude. The initial wind speed of the weather sequences does not evidently show any impact on those consequence indicators.

(3) Bin09 through Bin12

The calculation results for these weather bins that belong to atmospheric stability class E are shown in Figures 9 through 12. The estimation results of EF1k vary from 0 to several hundreds, and the portion of zero EF1k in Bin09 is apparently greater than that in the other bins. The estimation results of LC10 and LC1k scatter in the range of three orders of magnitude.

(4) Bin13 through Bin16

This group of bins is related to the most stable initial atmospheric stability class F and the calculation results are shown in Figure 13 through 16. Bin13 has some sequences of none early fatality, while others do not. The majority of EF1k values of the four bins falls in the range of 1 to100 cases, the highest being up to 600 cases. The values of LC10 and LC1k cover about three orders of magnitude with Bin16 as an exception. The distributions of LC10 and LC1k in Bin16 seem not so diverse as those of the 3 others in this group. The small specimen number may possibly be one of the reasons.

3.2.2 Wet weather bins

(1) Bin17 through Bin21

The calculation results of EF1k, LC10 and LC1k for Bins 17 through 21 are shown in Figures 17 through 21, respectively. These bins cover the wet weather sequences with the first precipitation intensity less than 2 mm/hr. All of them have a few sequences that result in high values of EF1k, for example over 400 cases. The values of LC10 vary from tens to thousands; while the values of LC1k vary in the range of thousands to tens of thousand.

According to the wet bin classification algorithm, the spatial interval where the plume segment reaches the first rainfall becomes further when the bin number increases. The influence of spatial interval is not remarkable on the consequence indicators chosen in this study.

(2) Bin22 through Bin26

The weather bins in this group are related to the intensity of the first rainfall between 2 and 4 mm/hr. The estimation results for them are shown in Figures 22 through 23, respectively.

The calculation results of EF1k for the four bins are below 100 cases except one sequence in Bin22, which is slightly greater than 100 cases. LC10 spreads in the range of 20 to 2,000 cases, varying within a factor of 100. The estimation results of LC1k change from 1,000 to about 500,000 cases, within a factor of 500. It seems that there is no striking influence of the spatial interval on the consequence indicators.

(3) Bin27 through Bin31

The total number of weather sequences in this group of bins is only 33, and there is no weather sequence in Bin28 for the conditions studied. Therefore, it is quite difficult to make any sound conclusions for these bins, which are related to rain intensity ranging from 4 to 6 mm/hr. By having compared with the results for the bins related to rain intensity of 2 to 4mm/hr, one might notice that the portion of LC1k greater than 10,000 cases increased with rain intensity. However, the calculation results EF1k and LC10 do not show any notable change when the intensity of the first rainfall increased.

(4) Bin32 through Bin36

Bin32, Bin33, Bin34, Bin35 and Bin36 are related to "heavy rain", the first rainfall being heavier than 6 mm/hr. These bins are also minor ones, and Bin33 only has 1 weather sequence. The spatial intervals become further away from the release point when the bin number increases according to the bin descriptions for these bins. It can be seen from Figure 24 that the further the plume segment met the first rainfall the less the EF1k. Compared to the results of bins of lighter rainfall, the portion of LC10 higher than 100 cases diminishes remarkably. The inter-bin change of LC1k is not notable within this group, and nor does the inter-group variation.

3.3 Variations of some statistical parameters

3.3.1 Variation of the bin average

The variation of the averages of the three consequence indicators is shown in Figure 25 for every bin. The bin average of EF1k varies more remarkable than the ones of LC10 and LC1k. Three marked characteristics of the bin average EF1k can be seen from this figure. Firstly, the EF1k becomes greater for dry sequence bins when the atmospheric stability class upgrades from A and B toward F. The higher air concentration at more stable atmospheric condition may be one important reason for this. Secondly, the EF1k is curtailed when the distance at which the plume segment meet the first rainfall becomes further away from the release point, especially in the case of heavy rains. Since the air concentration decreases rapidly when the plume moves, the chance will diminish for wet deposition to result in individual doses high enough to cause early fatality. Thirdly, the increase of rain intensity and the reduction of bin average of EF1k concurred for the wet weather bins. This seems quite strange. However, if we look into the meteorological file, it is easy to find that heavy rain were almost always coincident with strong wind which diluted the radioactive materials released to the atmosphere effectively and reduce the chance of high ground level air concentration. The occurrence probability and magnitude of early fatality is apt to be diminished by this coincidence. It should be pointed out that the bin average of EF1k did not change remarkably from Bin05 to Bin31. Hence, the weather bin categorization scheme should be modified in such a way that weather bins have notable different consequences.

The bin average of LC10 in dry conditions does not fluctuate so roughly as the bin average of EF1k does. It should be noticed that the numbers of weather sequences are small for most of the wet bins so the average values of LC10 or EF1k have relatively large uncertainties in these bins. The relatively weak fluctuation of the average LC10 illustrates that some environment factors other than initial wind speed and stability class should be taken into account in the bin classification schemes.

It is also illustrated in Figure 25 that the average of LC1k does not vary remarkably except at Bin08 and Bin17. However, the contribution of wet deposition to LC1k can be seen easily. If relatively sharp differences of LC1k are expecting to take place, such indices as initial wind speed, initial stability class and intensity of first rainfall should perhaps be replaced by time- integrals of those variables.

3.3.2 Variation of the maximum

It is shown in Figure 26 that the maximum of EF1k fluctuates more violently than those of LC10 and LC1k. Actually, accident consequence is a concept of multiple attribute features. We can not expect that all the attributes vary in perfect harmony.

The peak of bin maximum EF1k is located in Bin13. Therefore, more attention should be given to extremely stable atmospheric conditions with low wind speed, so that a complete spectrum of the accident consequence could be acquired.

3.3.3 Variation of the median

The variation of the median values of EF1k, LC10 and Lc1k are illustrated in Figure 27. The ranges of LC10 and LC1k median values are even narrower than ranges of the average values.

3.3.4 Variation of the minimum

It is shown in Figure 28 that only weather bin has its minimum EF1k value higher than 1, where the number of weather bin is one. The minimum values of LC10 and LC1k do not change remarkably. However, the contribution of wet deposition to LC1k can be seen from Bin17 through Bin36.

3.3.5 Variation of the percentiles

The calculation results of the 90 percentiles of EF1k, LC10 and LC1k are shown in Figure 29. Two peaks of EF1k can be seen at Bin13 and Bin17. The first one is related to extremely stable atmospheric condition and low wind speed. The second peak resulted partly from wet deposition in the vicinity of the postulated release point. It should be noticed that heavier rain does not mean higher EF1k. In dry bins, the LC10 and LC1k varied synchronously.

Figure 30 and Figure 31 show the calculation results for the 95 and 99 percentiles of EF1k, LC10 and LC1k, respectively. The variation of 95 and 99 percentiles are similar to those of the 90 percentiles. It should be pointed out that the 99 percentiles are not valid for some minor weather bins due to their members being too few.

3.3.6 Band width of different consequences

The maximum and minimum values of EF1k are shown together in Figure 32. It is obvious that the bands of EF1k of the bins are overlapped. This is completely not what was expected for the weather bin categorization scheme. The consequence of bin covers those of all the others. The widest band of EF1k is located at Bin14, which has 759 weather sequences. If a few sequences are sampled randomly from this bin, the rare case leading to the most severe consequences will normally be overlooked.

The band variation of LC10 and LC1k are shown in Figures 33 and 34, respectively. Band overlapping occurs for both LC10 and Lc1k as well. For example, the band of LC1k is widest at Bin06 and covers the range of LC1k for all the other bins.

4. CONCLUSIONS

Intensive calculations were made using the specific conditions provided by the MACSS code. Therefore, this work is a case study and the results and remarks presented in this paper are related to these specific conditions. Calculations for other sites or other conditions are apt to produce various results and lead to some different conclusions. It is possible, however, to include general findings about other accidents and other sites by reference to the results presented here. The conclusions based on the calculations of this work are given below:

(1) The sensitivities of different radiological consequences to the changes of weather bins are noticeably large. The adoption or construction of a sampling scheme must be tailored to the consequence of uppermost importance in the study being conducted.

(2) For a given initial wind speed in dry weather bins, early fatality is liable to increase synchronously with the initial atmospheric stability class.

(3) For a given initial stability class, early fatality has a tendency of decline when initial wind speed upgrades. Atmospheric stability class should be one factor to be considered with other factors in adopting a sampling scheme.

(4) Early fatality is not necessarily proportional to the precipitation intensity. Heavy rain conditions caused higher contamination of the ground, on the other hand they were usually associated with strong winds that diluted the radioactive materials released to the atmosphere effectively.

(5) The bands of radiological consequences at one bin can be wide enough to cover those of all the others. In this work, the widest band is located at Bin14, which has 759 sequences. If a few sequences were randomly sampled from that bin, it would be more probable to overlook the rare adverse conditions than cyclic or random sampling method does.

(6) Early health effects are determined by absorbed doses received in a relative short period of time. Weather conditions are always changing, so time-integrals of meteorological parameters such as wind speed and atmospheric stability should be used instead of the initial ones.

(7) The wide spread of radiological consequences possibly demonstrates that population distribution should be taken into account in the procedures of categorization of weather sequences.

Acknowledgement

This work was supported by the Science and Technology Agency (STA) Scientist Exchange Program. The authors would like to express special thanks to Messrs. MURAMATSU Ken and KOBAYASHI Kensuke for their helps making this work be carried out successfully. We would like also to give our thanks to Messrs. KIDA Takashi and TOMITA Kenichi for their assistance in preparing the figures.

REFERENCES

[1] Freeman, R.I., Moir, G.R., "What is living PSA?", Nuclear Energy, 32(6), 355-362, 1993.

[2] USNRC, "Reactor Safety Study- An Assessment of Accident Risks in the US Commercial Nuclear Power Plants", WASH-1400, NUREG-75/014, 1975.

[3] OECD, "Probabilistic Accident Consequence Assessment Codes, Second International Comparison, Overview Report", Nuclear Energy Agency, 1994.

[4] Chanin, D.I., Sprung, J.L., Ritchie, L.T., Jow, H-N, "MELCOR Accident Consequence Code System (MACCS), User's Guide", NUREG/CR-4691 Vol. 1, 1990.

[5] Ehrhardt, J., Burkart, K., Hasemann, I., Matzerath, C., Panitz, H-j, and Steinhauer, C., "The Program system UFOMOD for assessing the consequences of nuclear accidents", KfK-4330, Kernforschungszentrum Karlsruhe, 1988.

[6] Clarke, R.H., Kelly, G.N., "MARC – the NRPB methodology for assessing the radiological consequences of accidental releases of activity", NRPB-R127, London HMSO, 1981.

[7] NRPB, "CONDOR 1:A Probabilistic Consequence Assessment Code Applicable to Releases of Radionuclides to the Atmosphere," NRPB-R258, London HMSO, 1993.

[8] Commission of the European Communities, "COSYMA: A new program package for accident consequence assessment", EUR 13028/EN, 1991.

[9] Homma, T., Togawa, O., Iijima, T., "Development of Accident Consequence Assessment Code at JAERI", in Proceedings of the "Seminar on methods and codes for assessing the off-site consequences of nuclear accidents", Athens, 7 to 11 May 1990, EUR 13013/2, p.1049-1063, 1991.

[10] IAEA, "Procedures for Conducting Probabilistic Safety Assessments of Nuclear Power Plants (Level3)", Safety Series No.50-P-12, STI/Pub/1009, 1996.

[11] Jow, H-N., Sprung, J.L., Rollstin, J.A., Tichie L.T., Channin, D.I., "MELCOR Accident Consequence Code System (MACCS), Model Description", NUREG/CR-4691 Vol. 2, 1990.

[12]Panitz, H.J., Matzerath, C., Pasler-Sauer, J., "UFOMOD Atmospheric Dispersion and Deposition", KfK-4332, Kernforschungszentrum Karlsruhe, 1989.

[13]Talleria, D.M., Salles, M. A., "Contribution of Meteorological sampling schemes to Uncertainty in PC COSYMA Calculations", in "Special Topics Related to Level-3 PSA/Dose Calculations", IAEA J4-TC-835.3, Vienna, 1997.

[14]Kim, D-H, private communication, JAERI, Tokai/Japan, 1998.

[15]Hasemann, I., Jones, J.A., Steen J. van der, Wonderen, E. van, "Experience with COSYMA in an international intercomparison of probabilistic accident consequence assessment codes", Nuclear Technology, 113, 291-303, 1996.

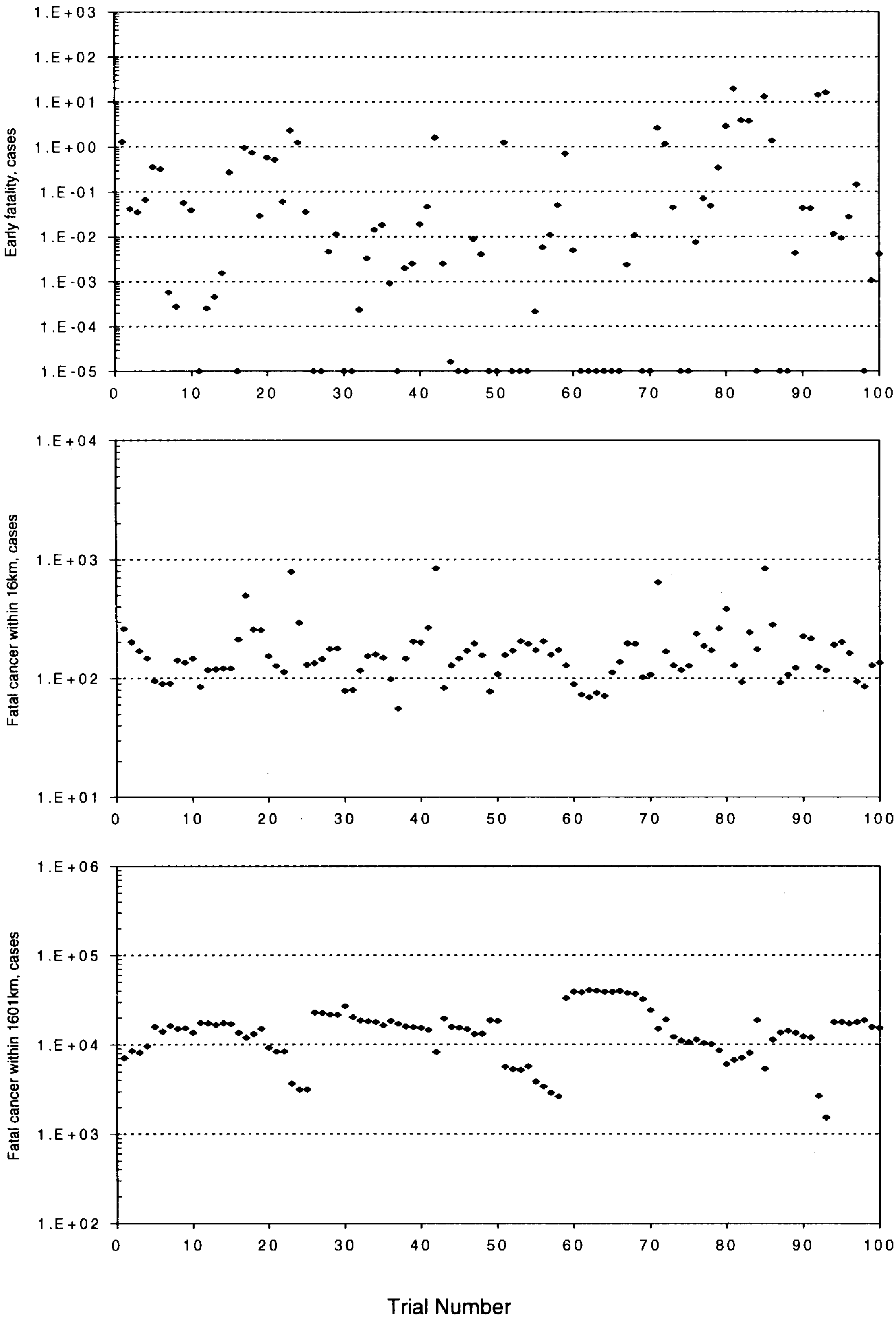

Figure 1. The variation of health effect estimation in BIN01. 100 weather sequences were seasonally sampled from the 957 weather sequences in BIN01.

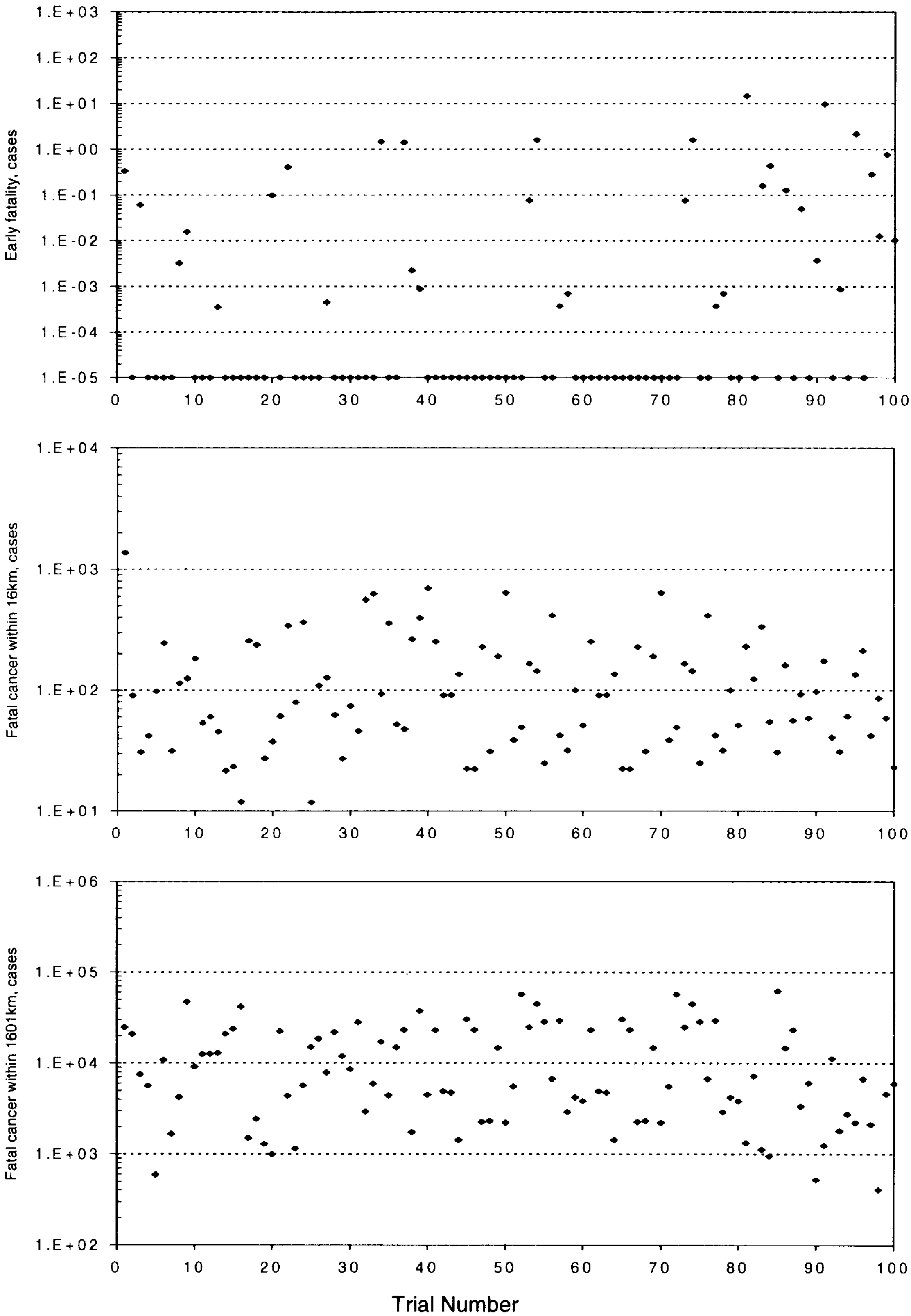

Figure 2. The variation of health effect estimation in BIN02. 100 weather sequences were seasonally sampled from the 946 weather sequences in BIN02.

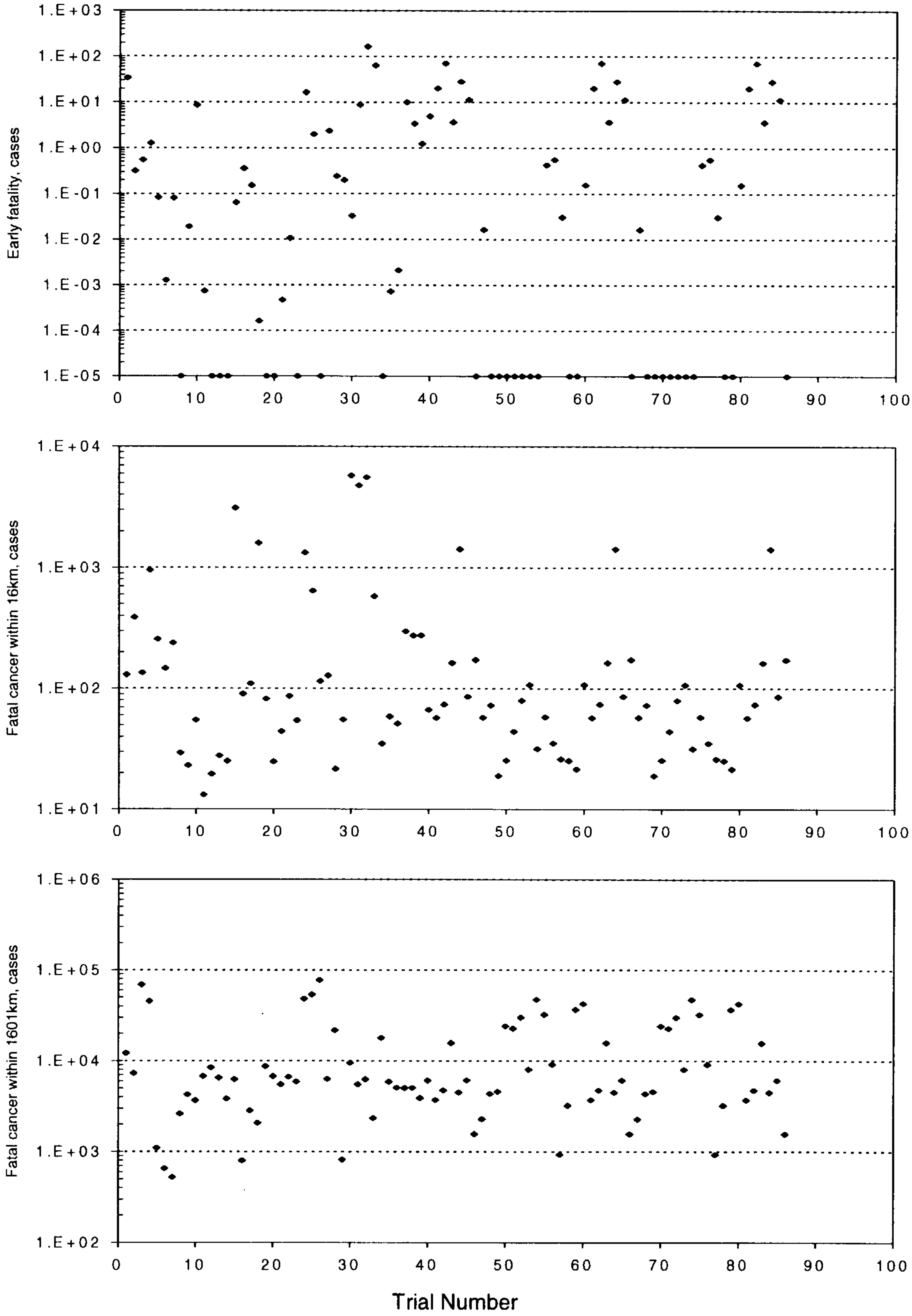

Figure 3. The variation of health effect estimation in BIN03. 86 weather sequences were seasonally sampled from the 86 weather sequences in BIN03.

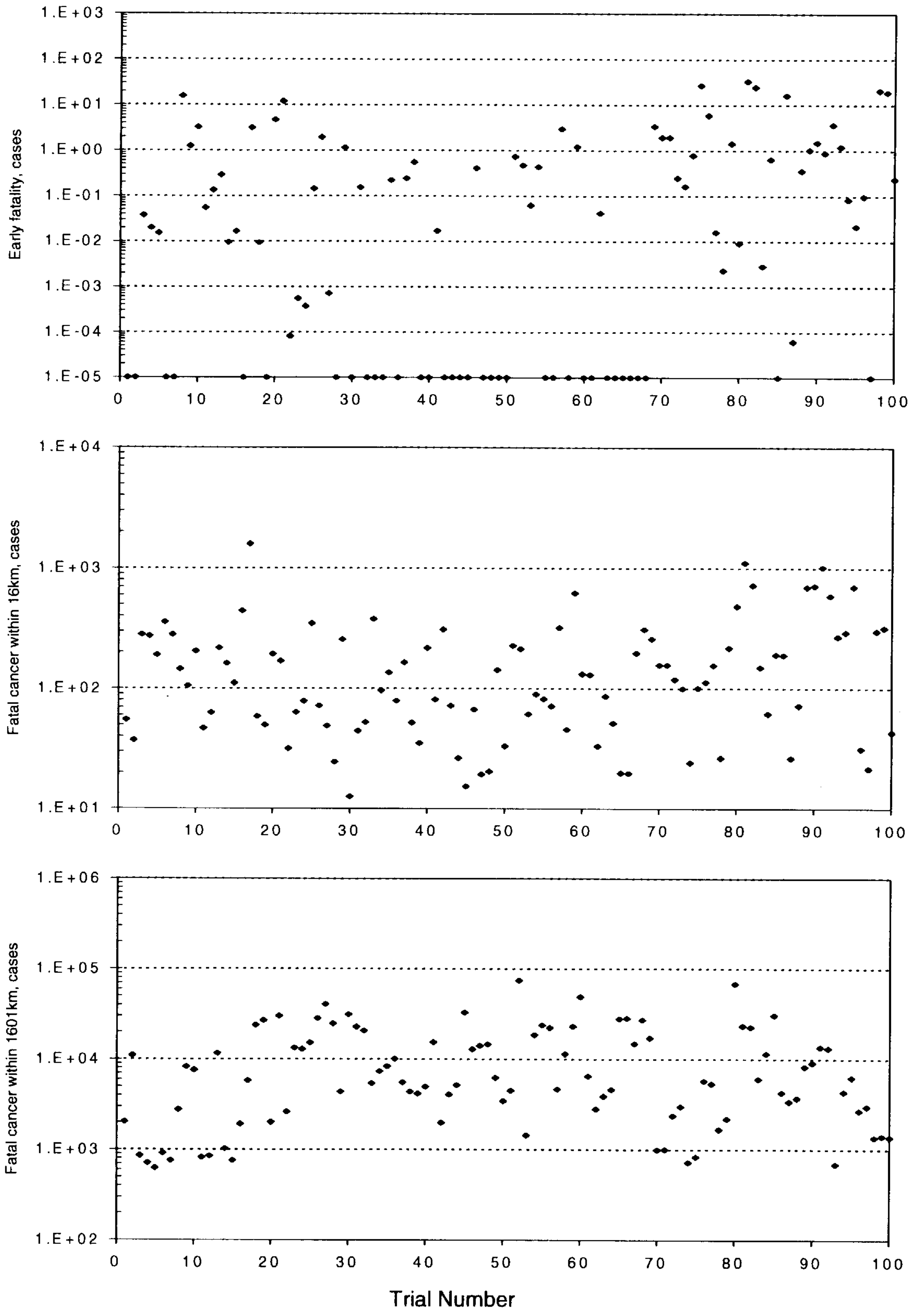

Figure 4. The variation of health effect estimation in BIN04. 100 weather sequences were seasonally sampled from the 572 weather sequences in BIN04.

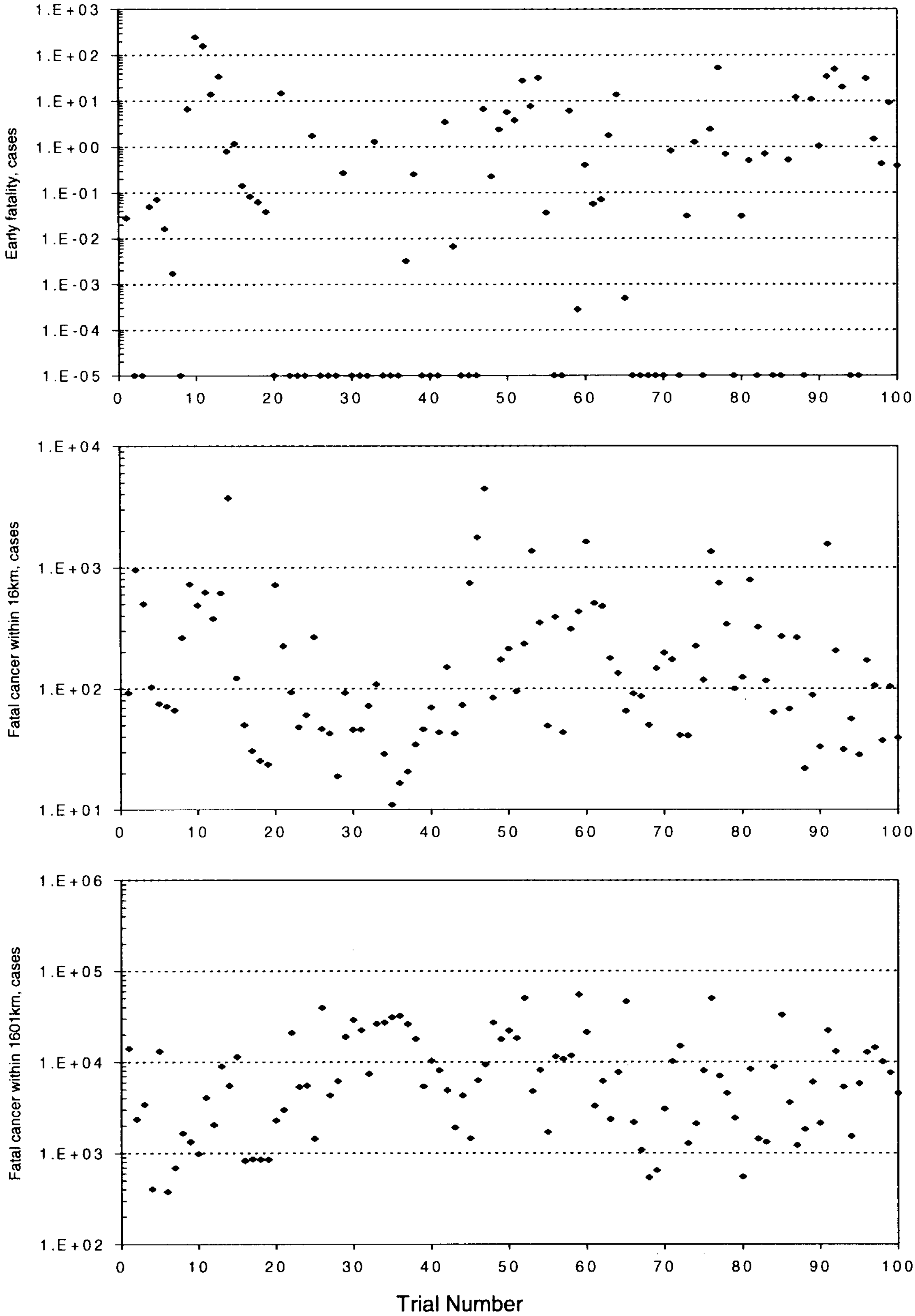

Figure 5. The variation of health effect estimation in BIN05. 100 weather sequences were seasonally sampled from the 544 weather sequences in BIN05.

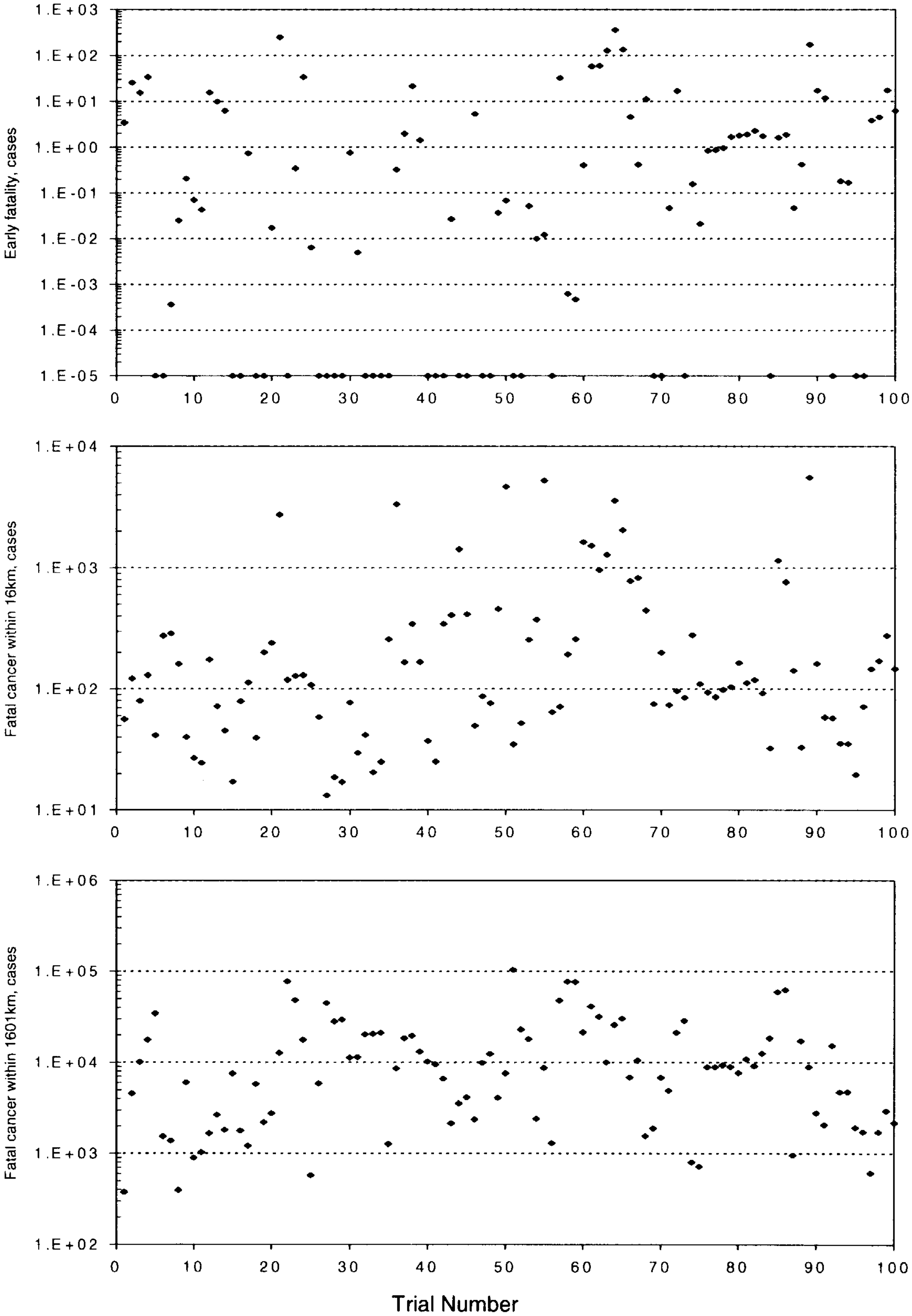

Figure 6. The variation of health effect estimation in BIN06. 100 weather sequences were seasonally sampled from the 658 weather sequences in BIN06.

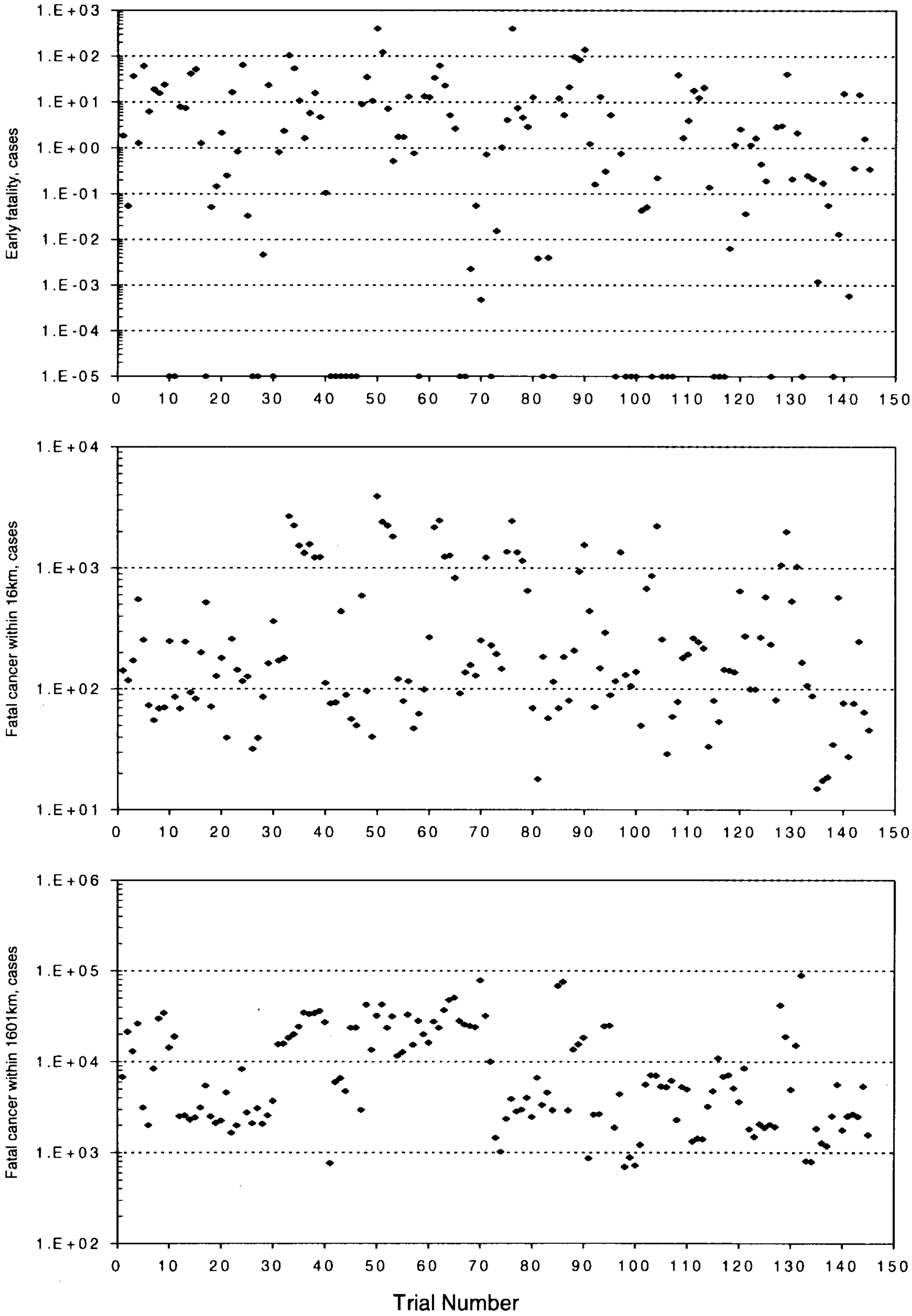

Figure 7. The variation of health effect estimation in BIN07. 145 weather sequences were seasonally sampled from the 145 weather sequences in BIN07.

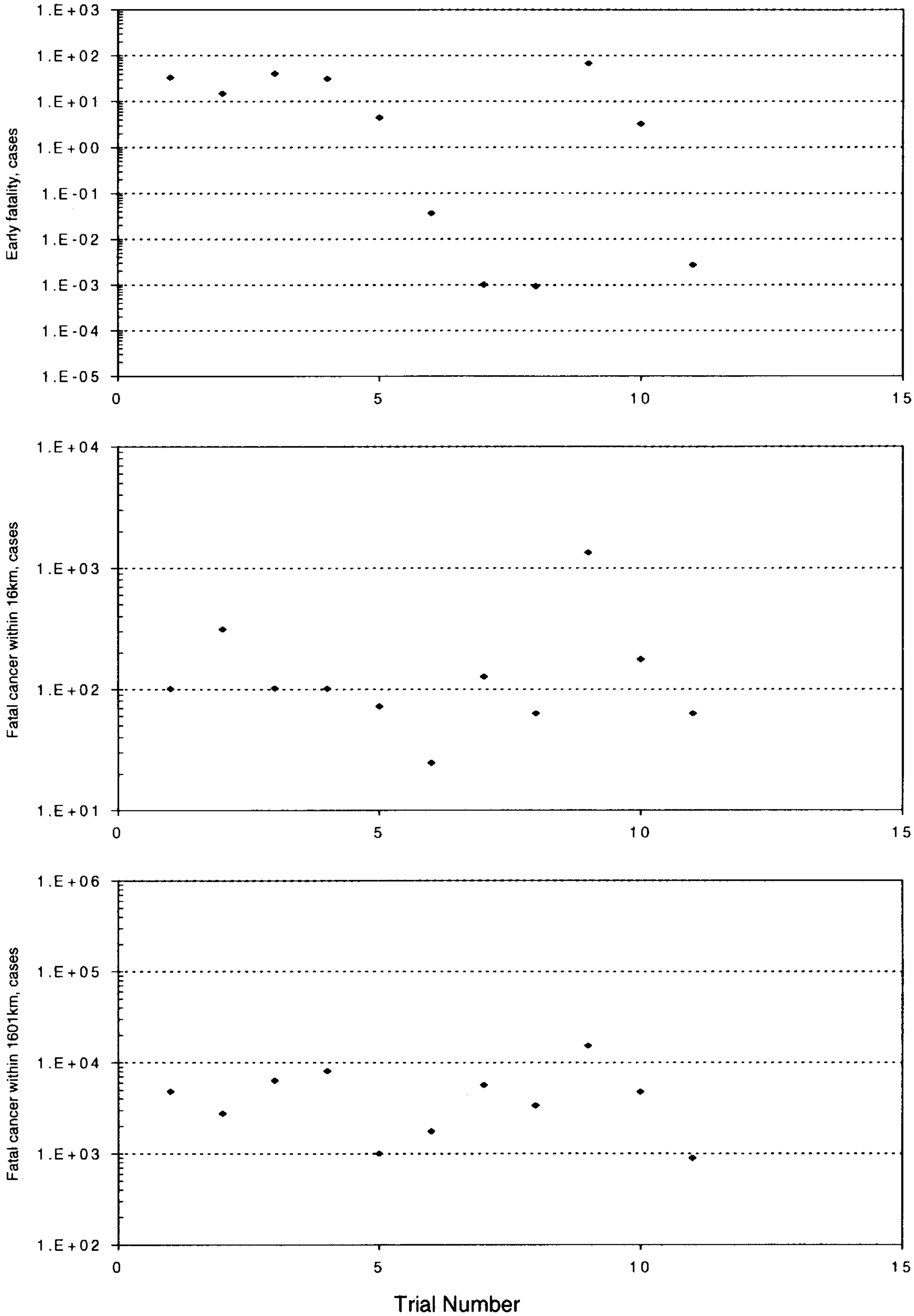

Figure 8. The variation of health effect estimation in BIN08. 11 weather sequences were seasonally sampled from the 11 weather sequences in BIN08.

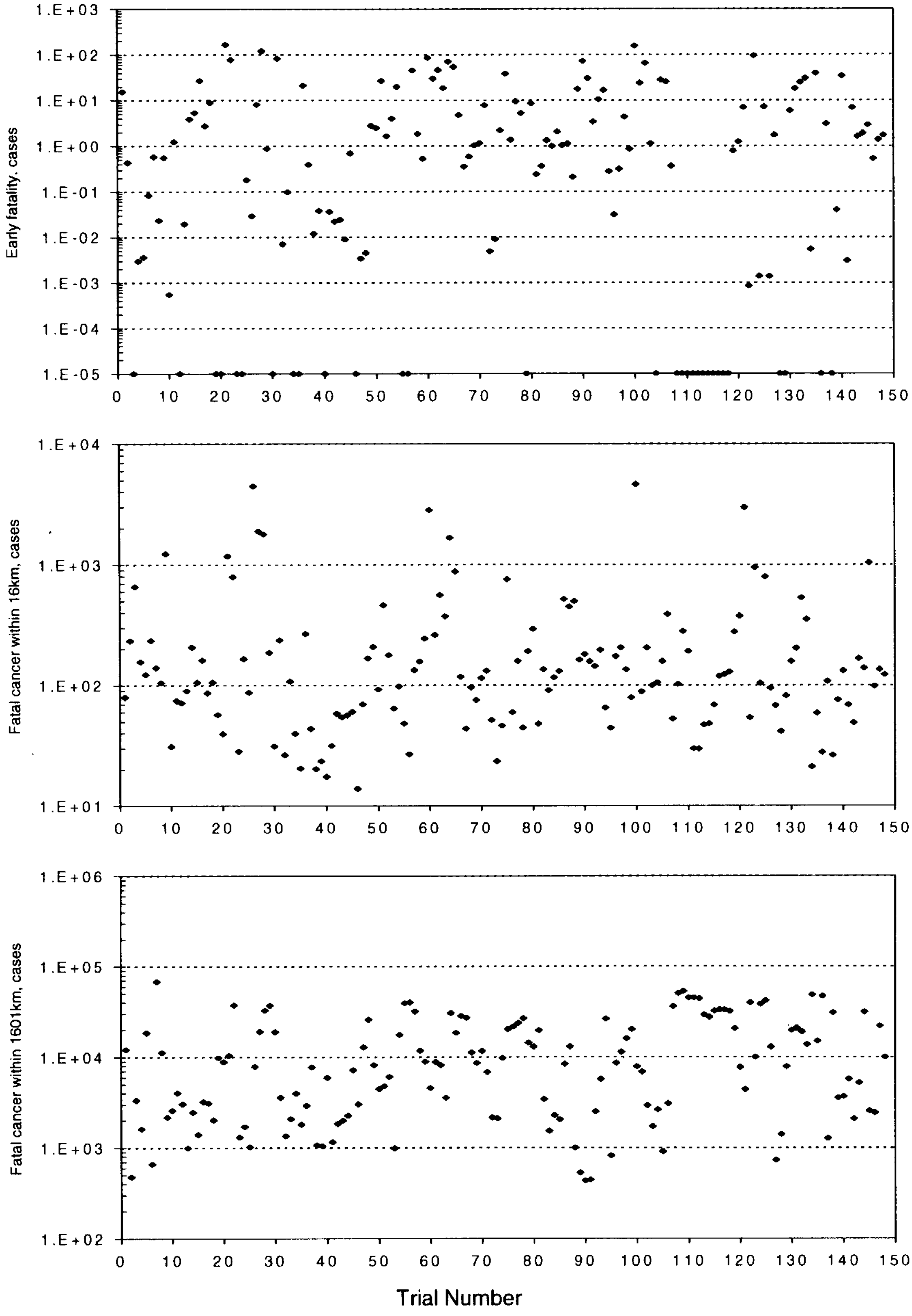

Figure 9. The variation of health effect estimation in BIN09. 148 weather sequences were seasonally sampled from the 148 weather sequences in BIN09.

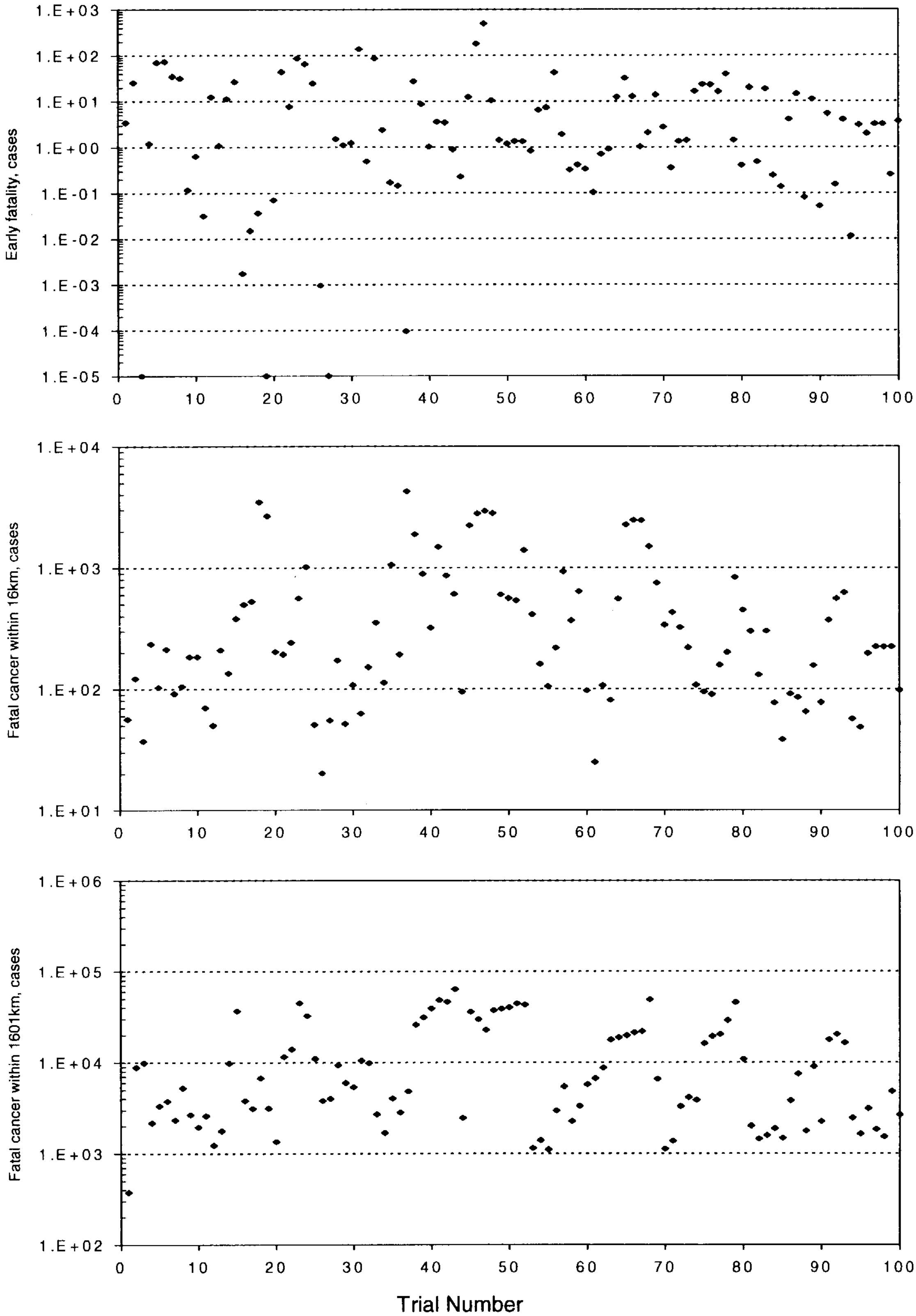

Figure 10. The variation of health effect estimation in BIN10. 100 weather sequences were seasonally sampled from the 668 weather sequences in BIN10.

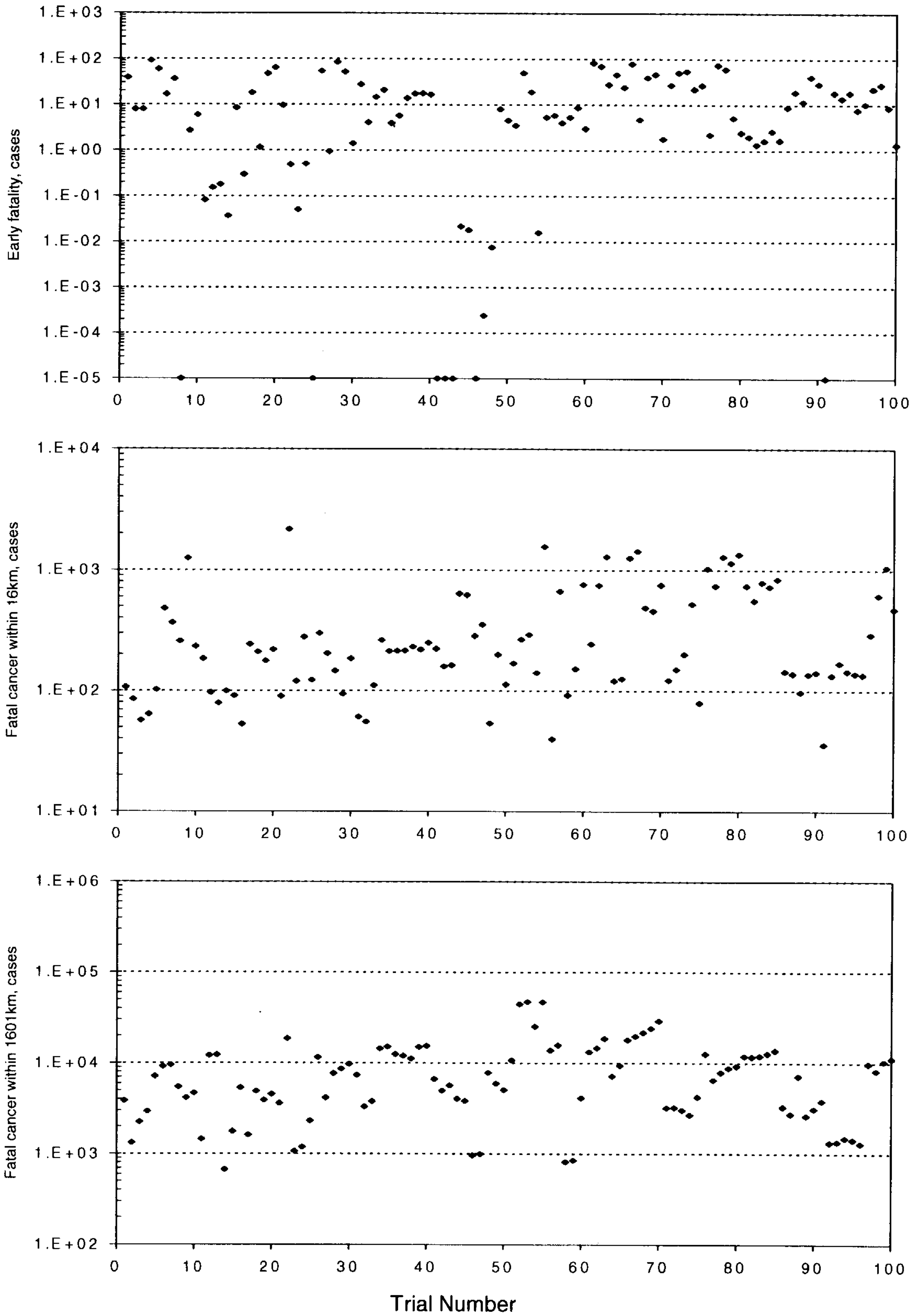

Figure 11. The variation of health effect estimation in BIN11. 100 weather sequences were seasonally sampled from the 758 weather sequences in BIN11.

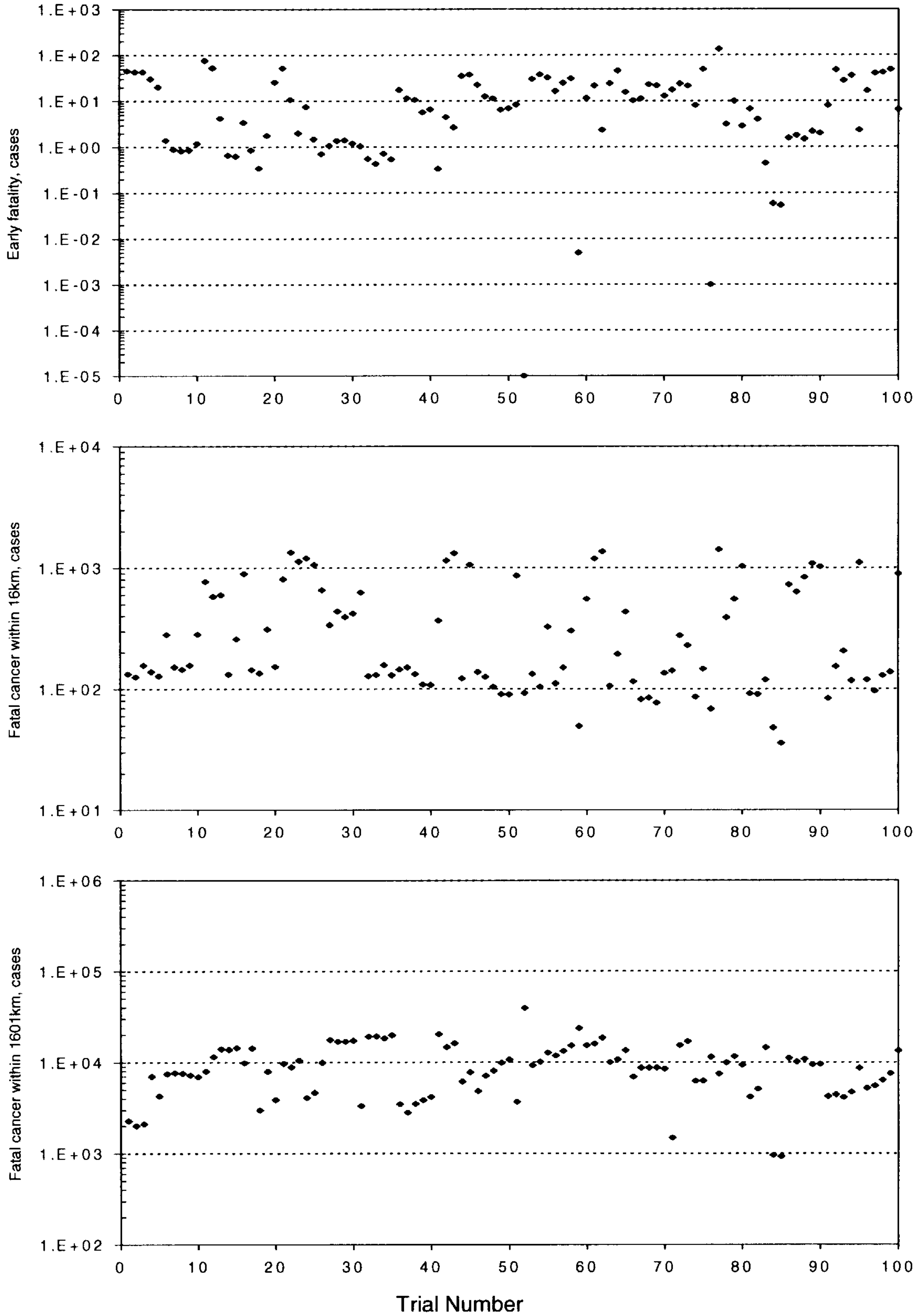

Figure 12. The variation of health effect estimation in BIN12. 100 weather sequences were seasonally sampled from the 599 weather sequences in BIN12.

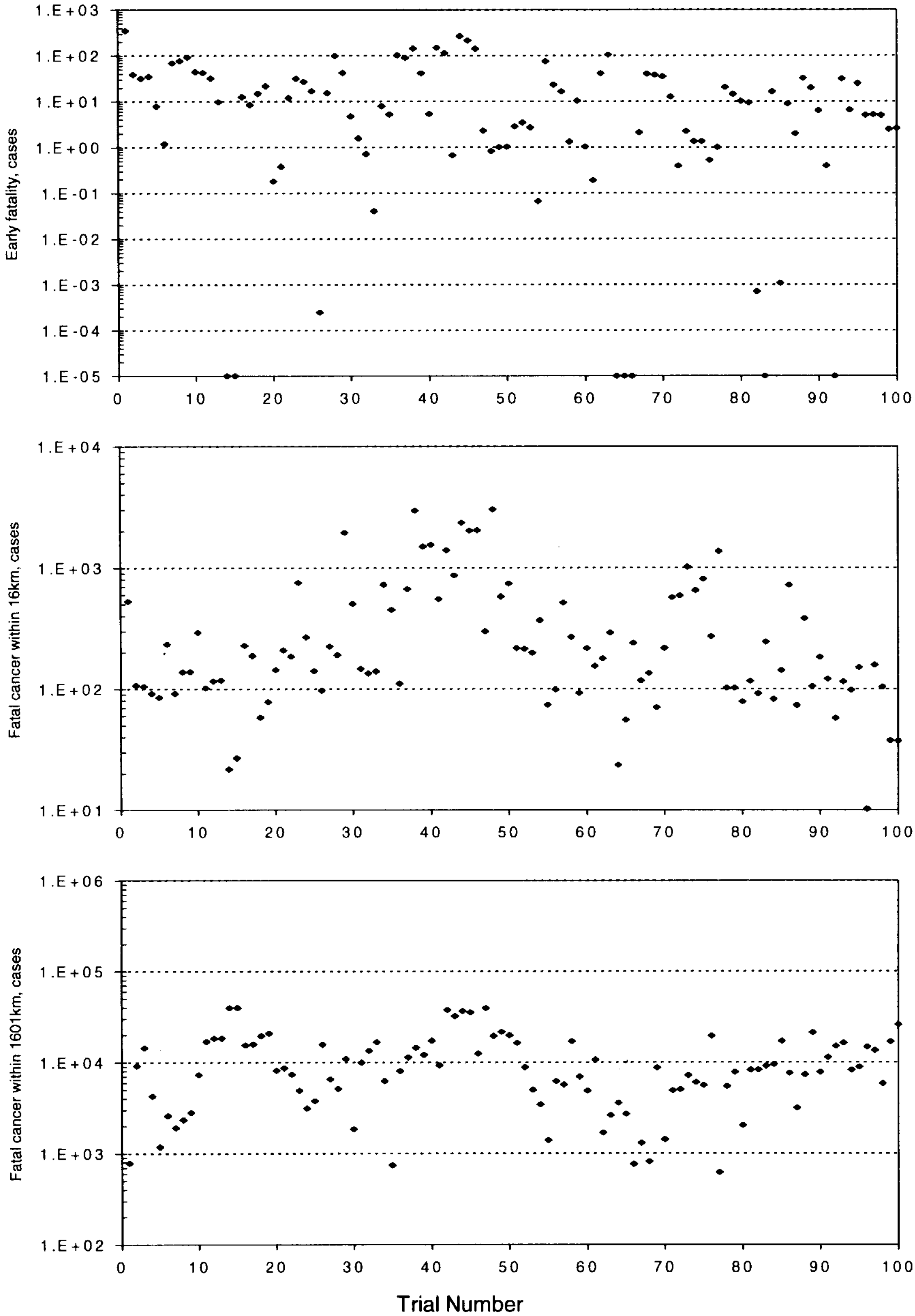

Figure 13. The variation of health effect estimation in BIN13. 100 weather sequences were seasonally sampled from the 774 weather sequences in BIN13.

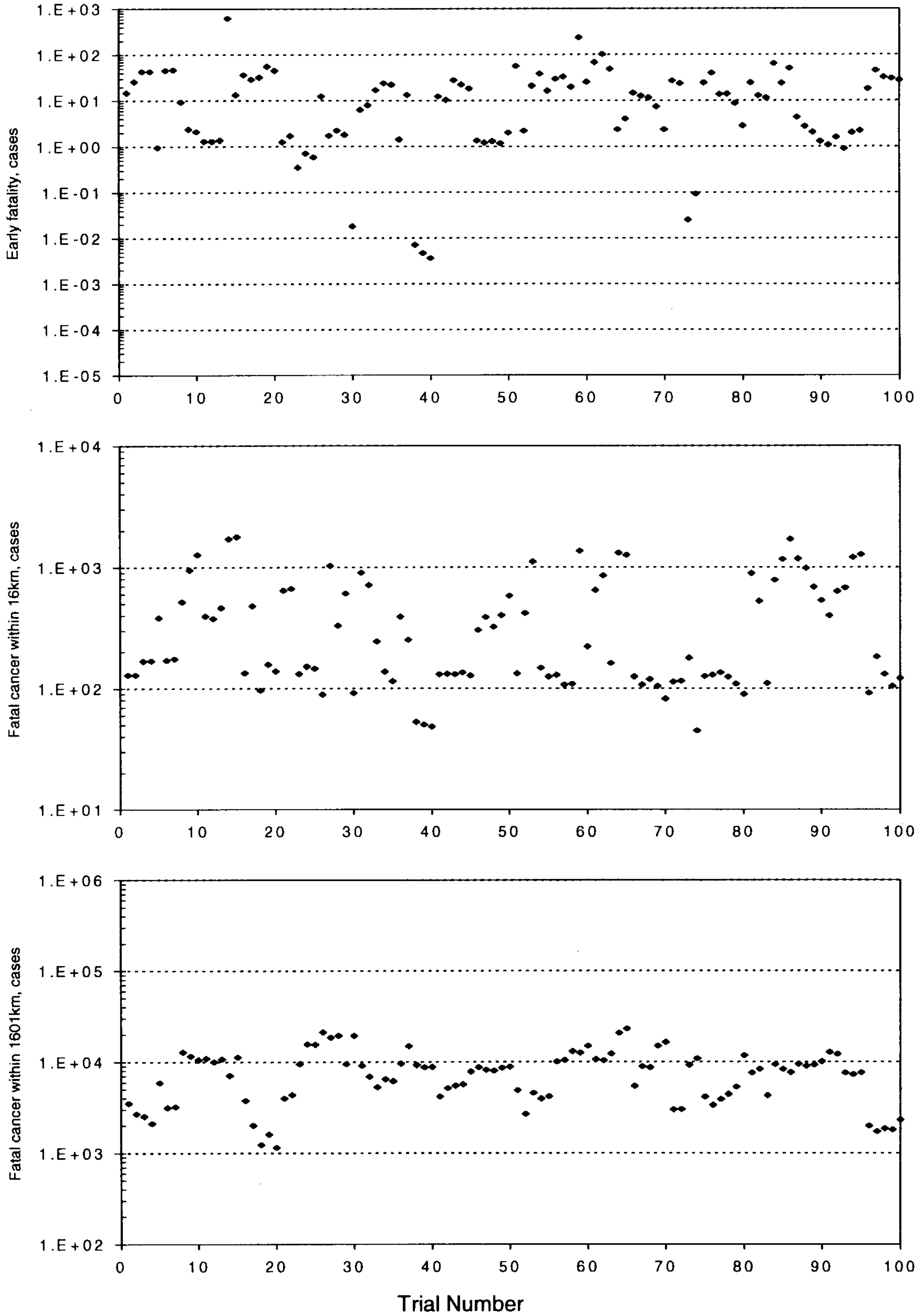

Figure 14. The variation of health effect estimation in BIN14. 100 weather sequences were seasonally sampled from the 759 weather sequences in BIN14.

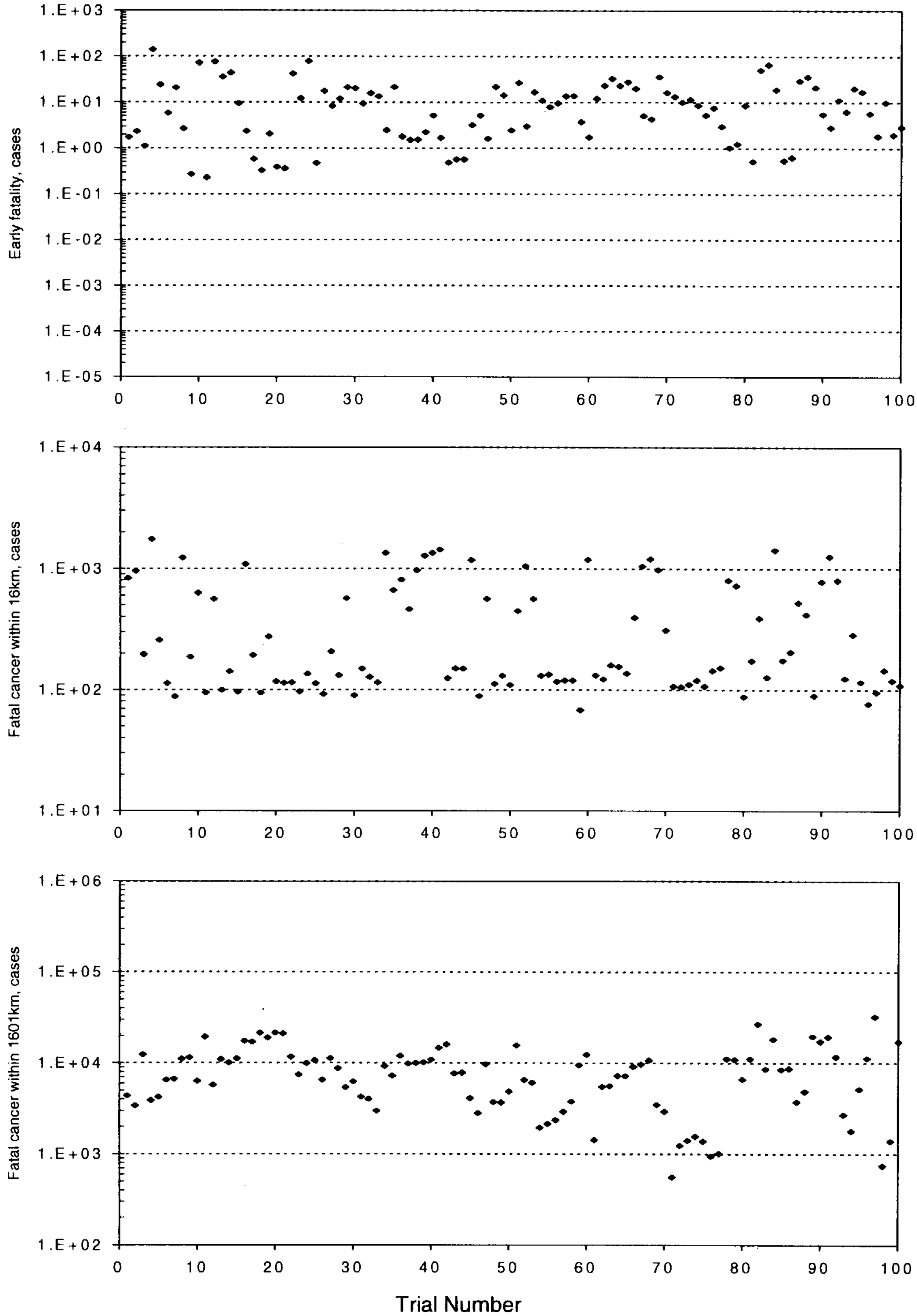

Figure 15. The variation of health effect estimation in BIN15. 100 weather sequences were seasonally sampled from the 145 weather sequences in BIN15.

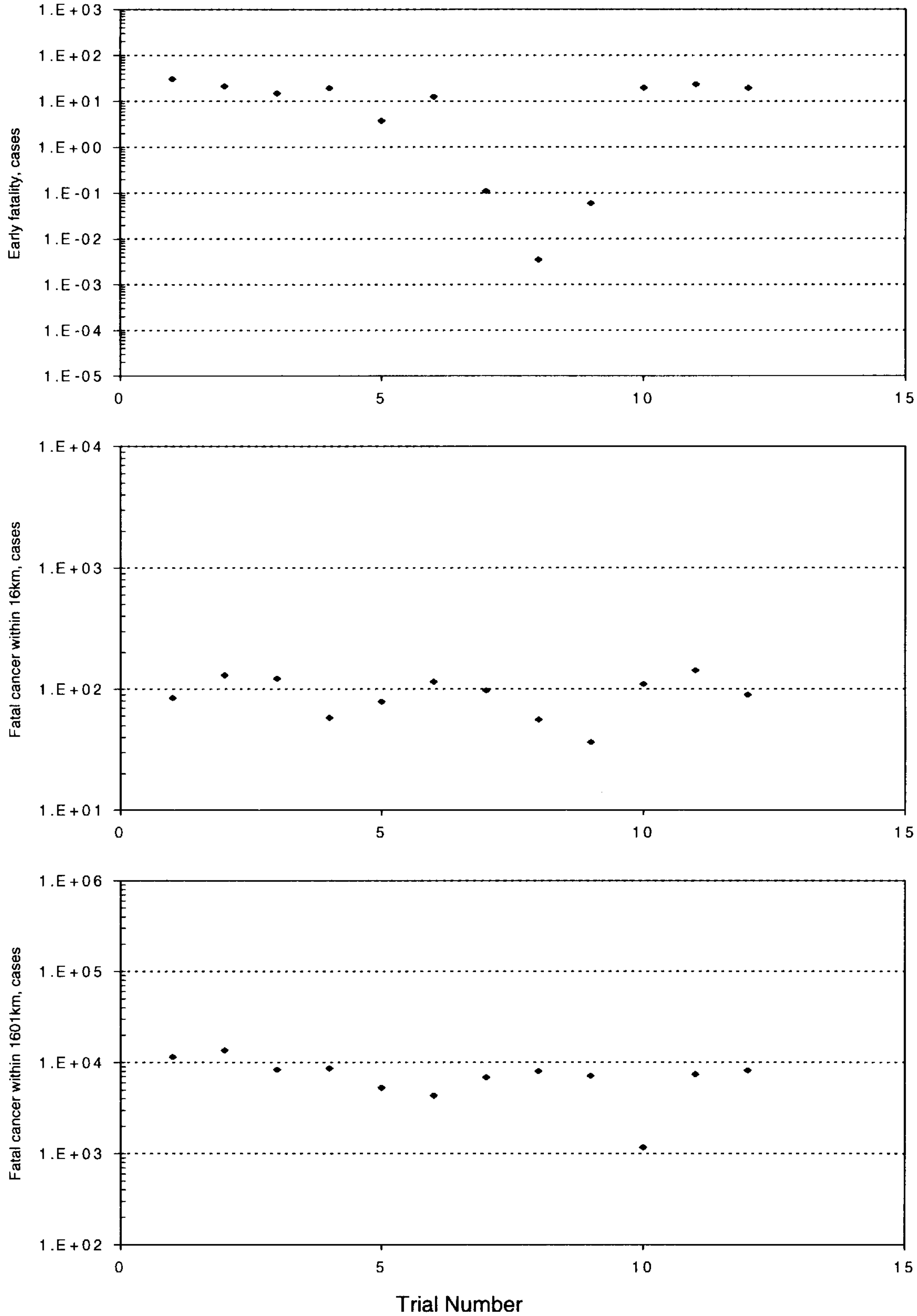

Figure 16. The variation of health effect estimation in BIN16. 12 weather sequences were seasonally sampled from the 12 weather sequences in BIN16.

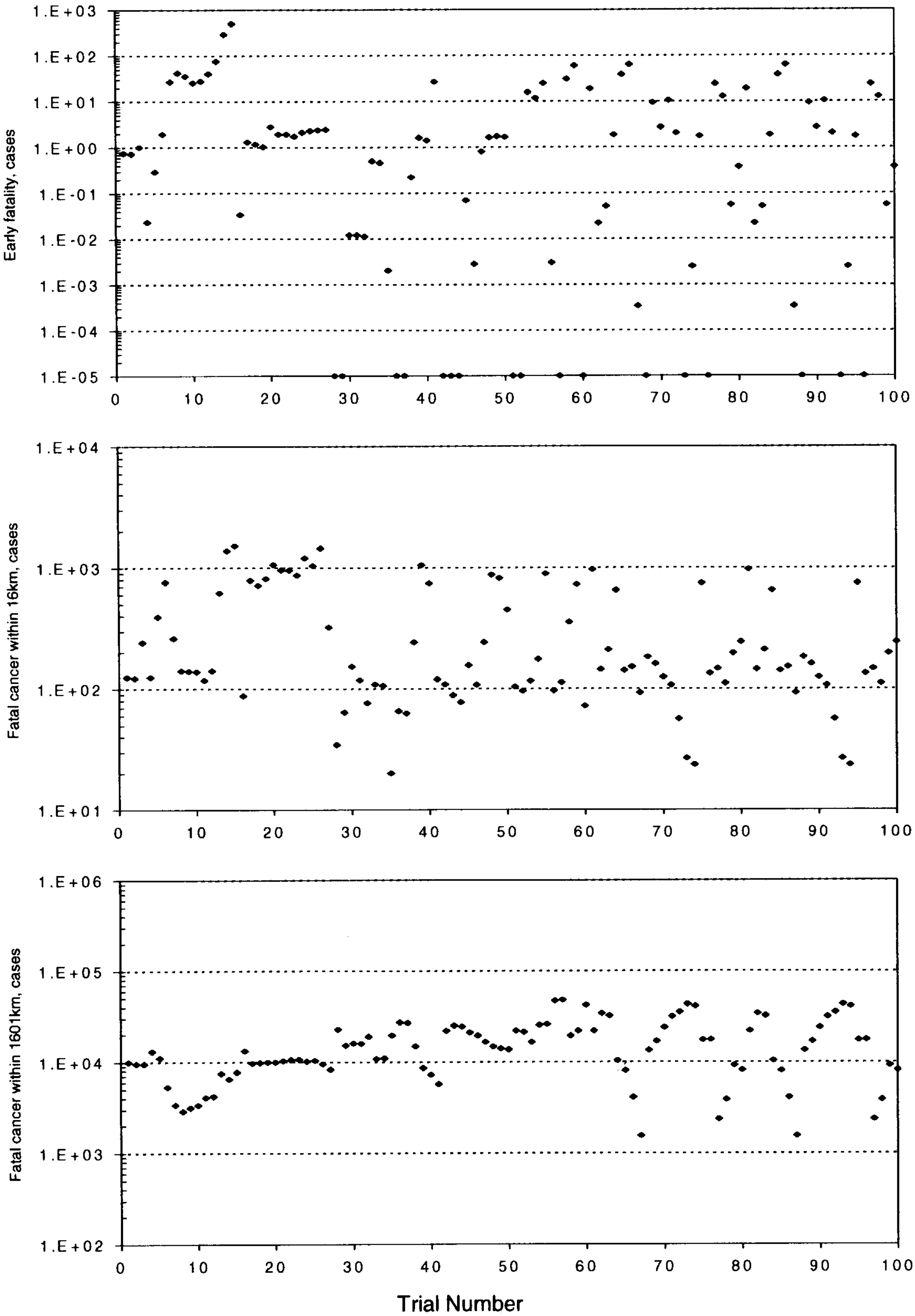

Figure 17. The variation of health effect estimation in BIN17. 100 weather sequences were seasonally sampled from the 352 weather sequences in BIN17.

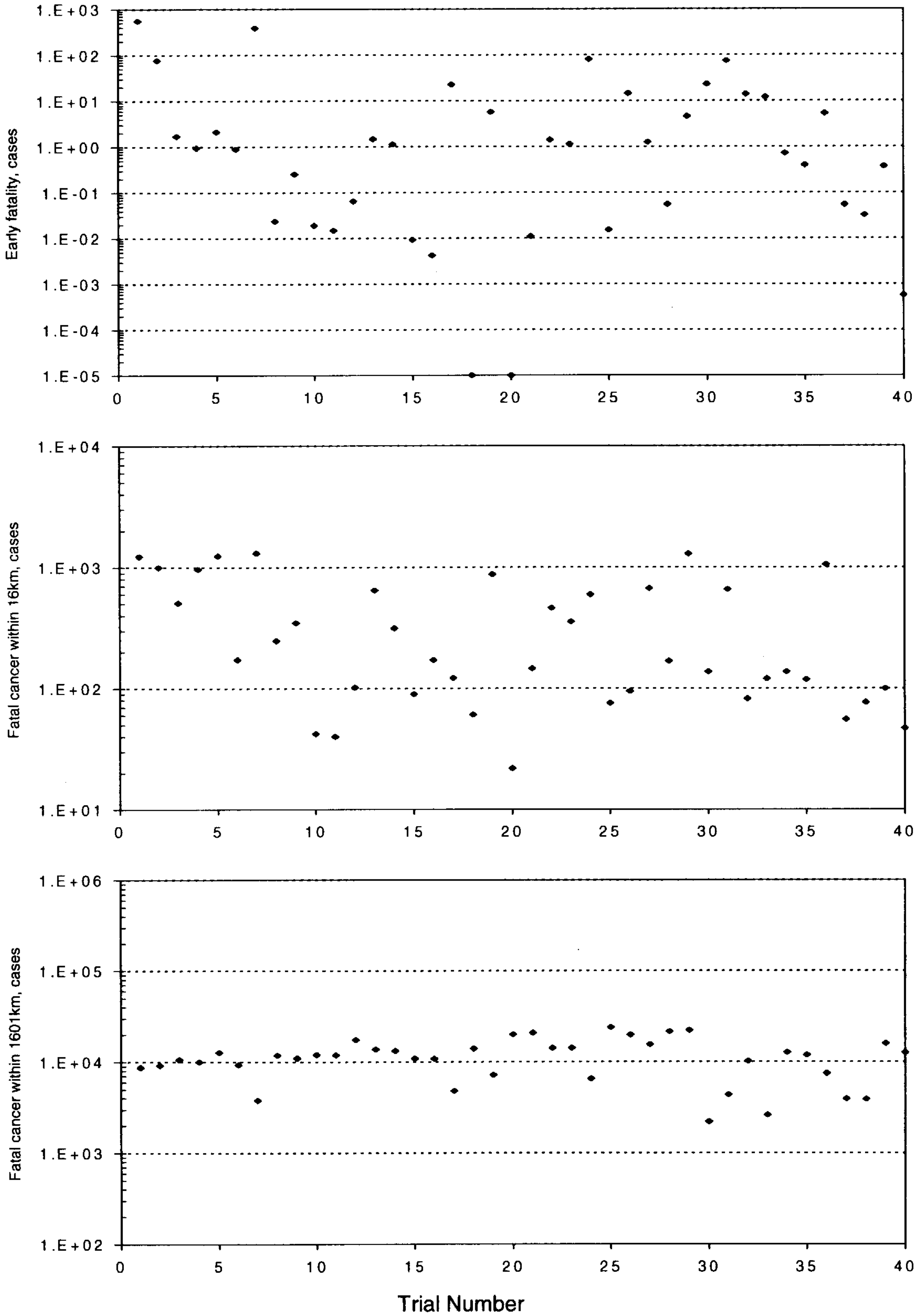

Figure 18. The variation of health effect estimation in BIN18. 40 weather sequences were seasonally sampled from the 40 weather sequences in BIN18.

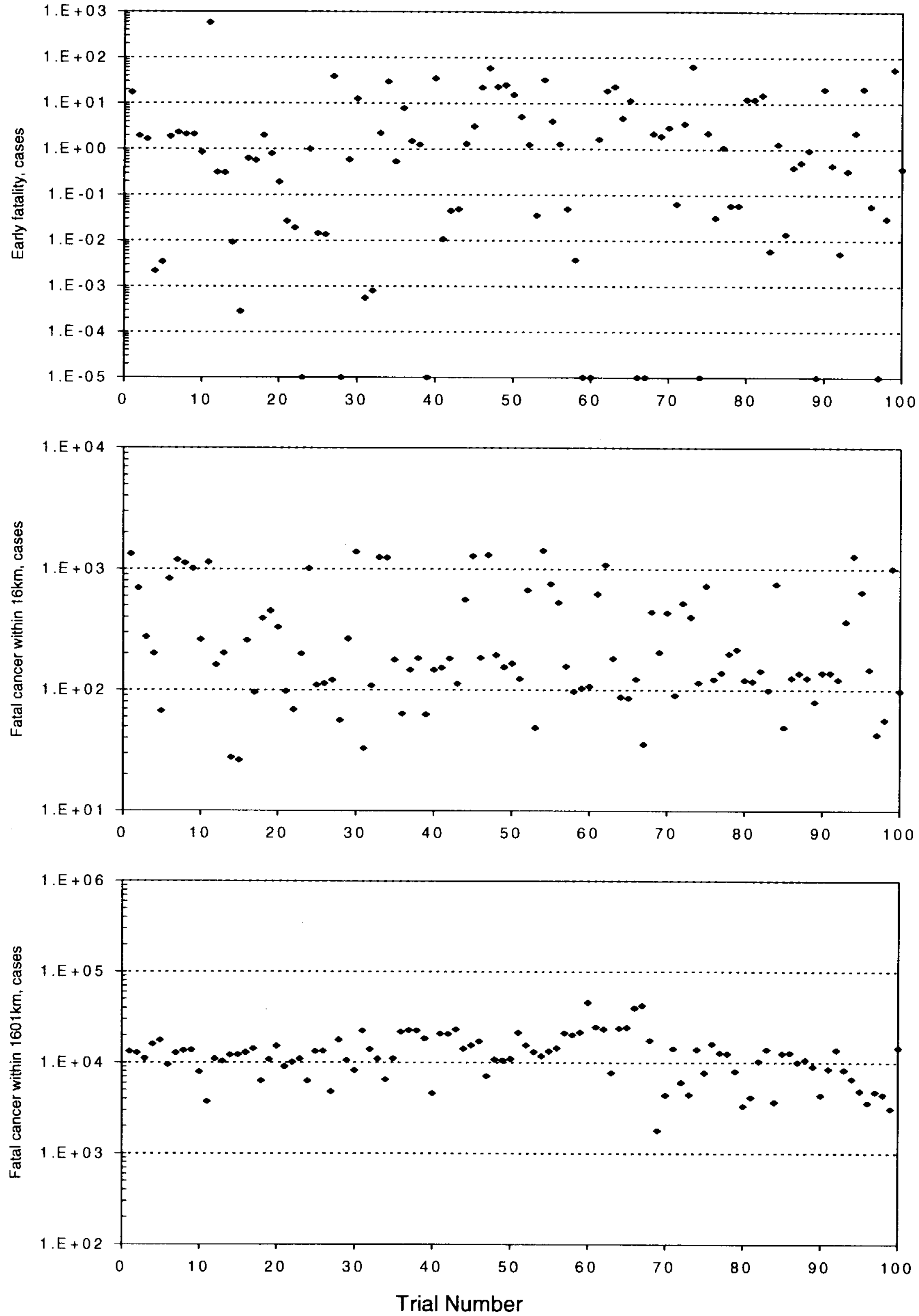

Figure 19. The variation of health effect estimation in BIN19. 100 weather sequences were seasonally sampled from the 103 weather sequences in BIN19.

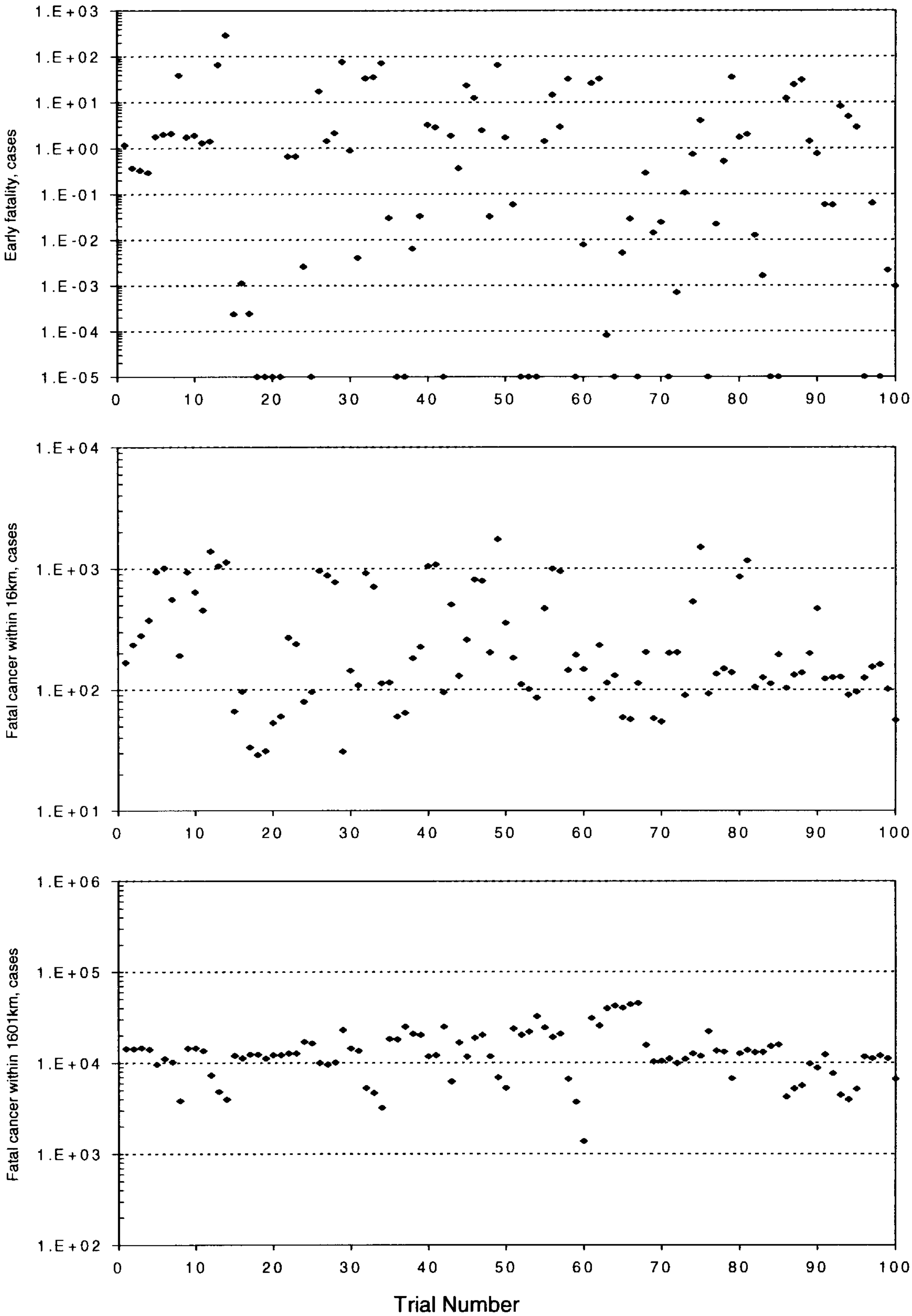

Figure 20. The variation of health effect estimation in BIN20. 100 weather sequences were seasonally sampled from the 132 weather sequences in BIN20.

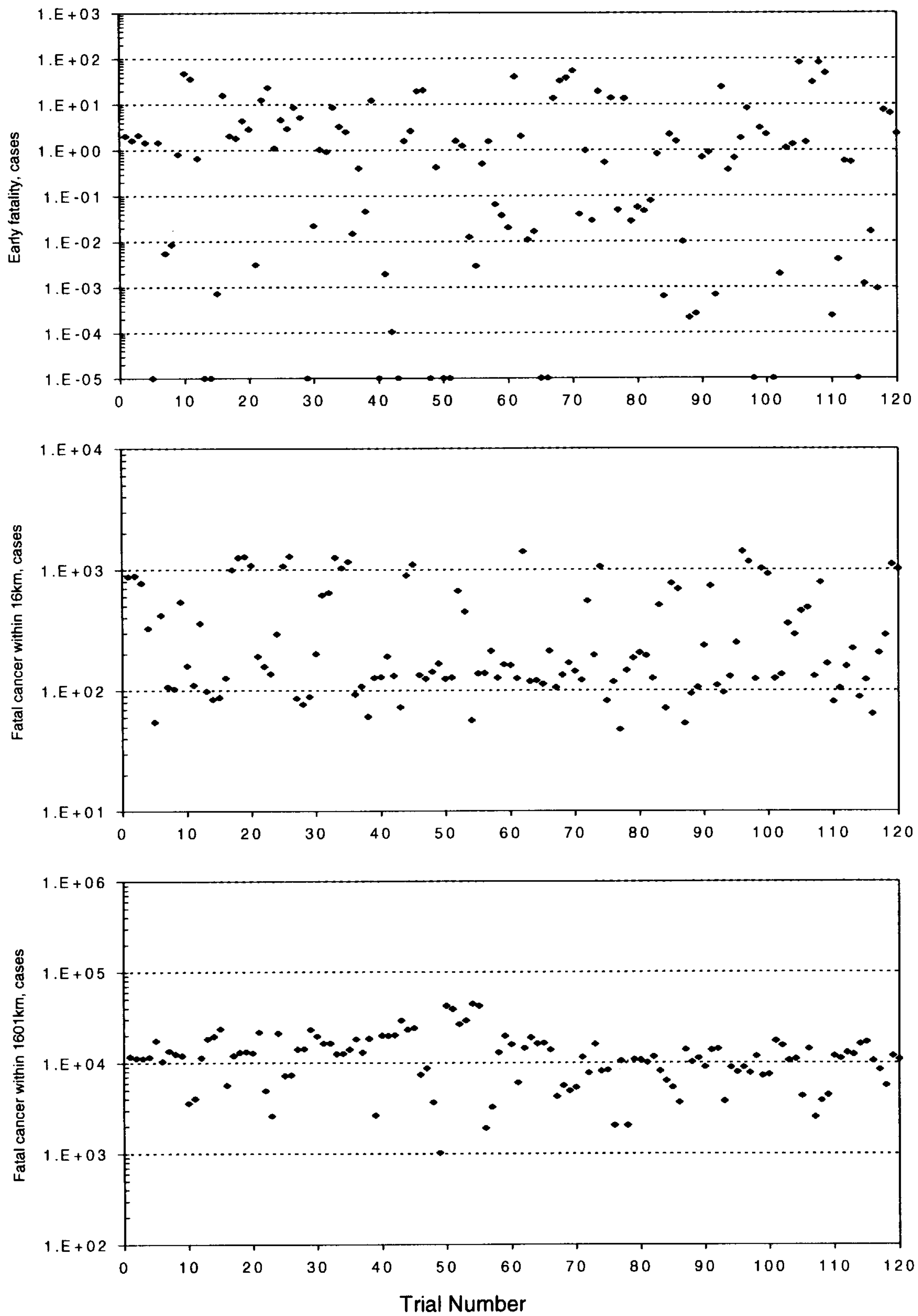

Figure 21. The variation of health effect estimation in BIN21. 120 weather sequences were seasonally sampled from the 127 weather sequences in BIN21.

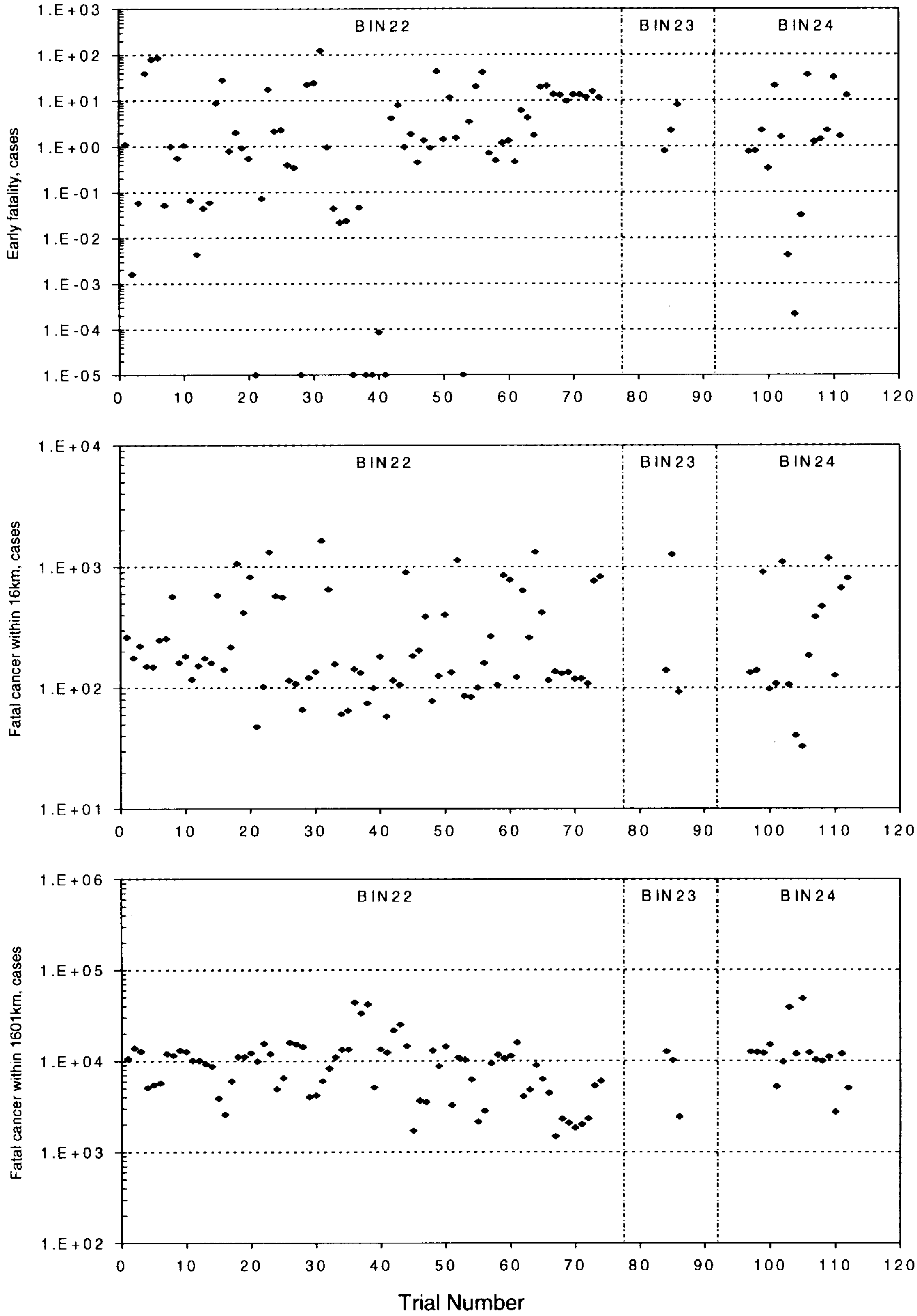

Figure 22. The variation of health effect estimation in BIN22, BIN23 and BIN24. 74, 3 and 16 weather sequences were completely sampled from BIN22, BIN23 and BIN24, respectively.

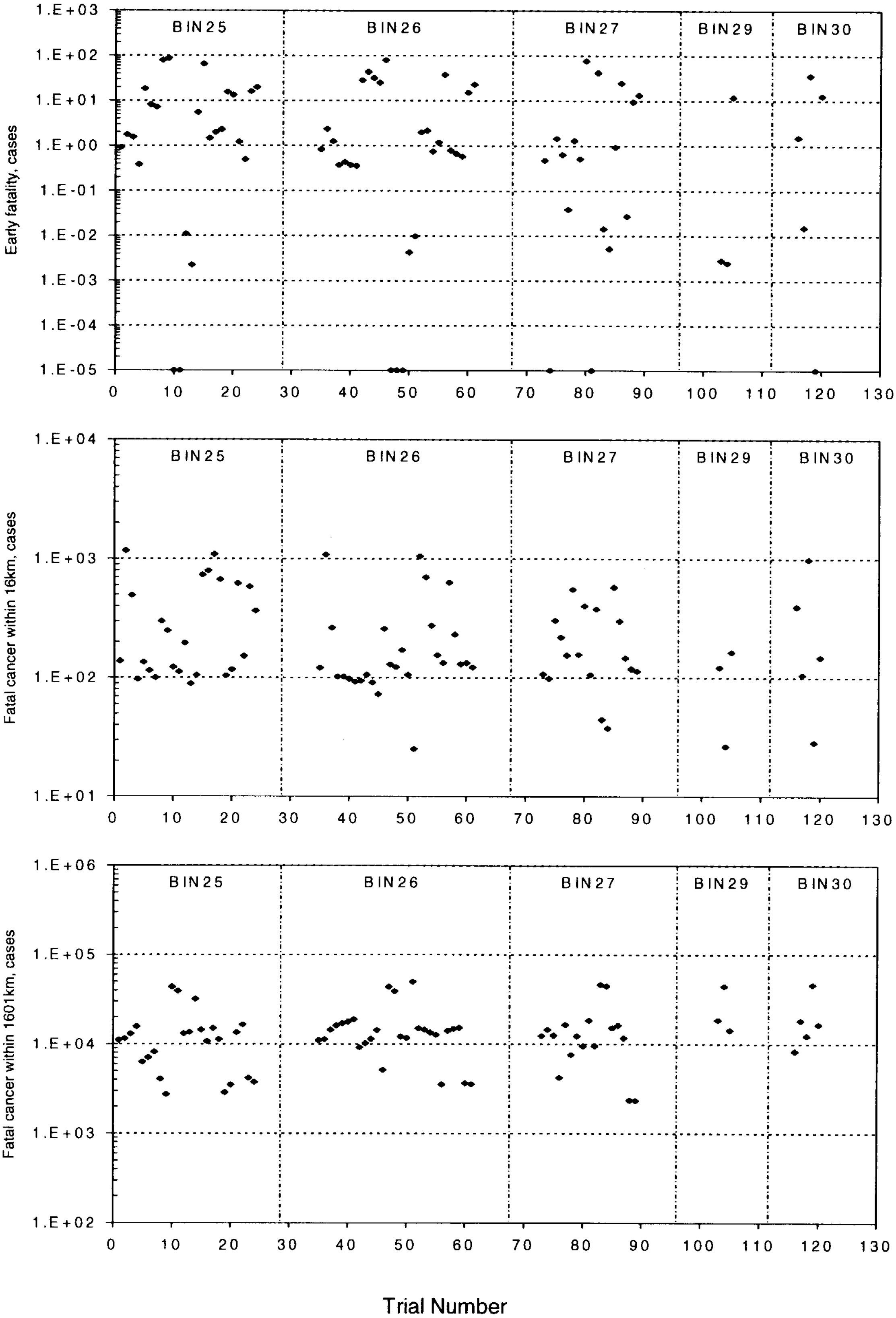

Figure 23. The variation of health effect estimation in BIN25, BIN26, BIN27, BIN29 and BIN30. 24, 27, 17, 3 and 5 weather sequences were completely sampled from BIN25, BIN26, BIN27, BIN29 and BIN30, respectively.

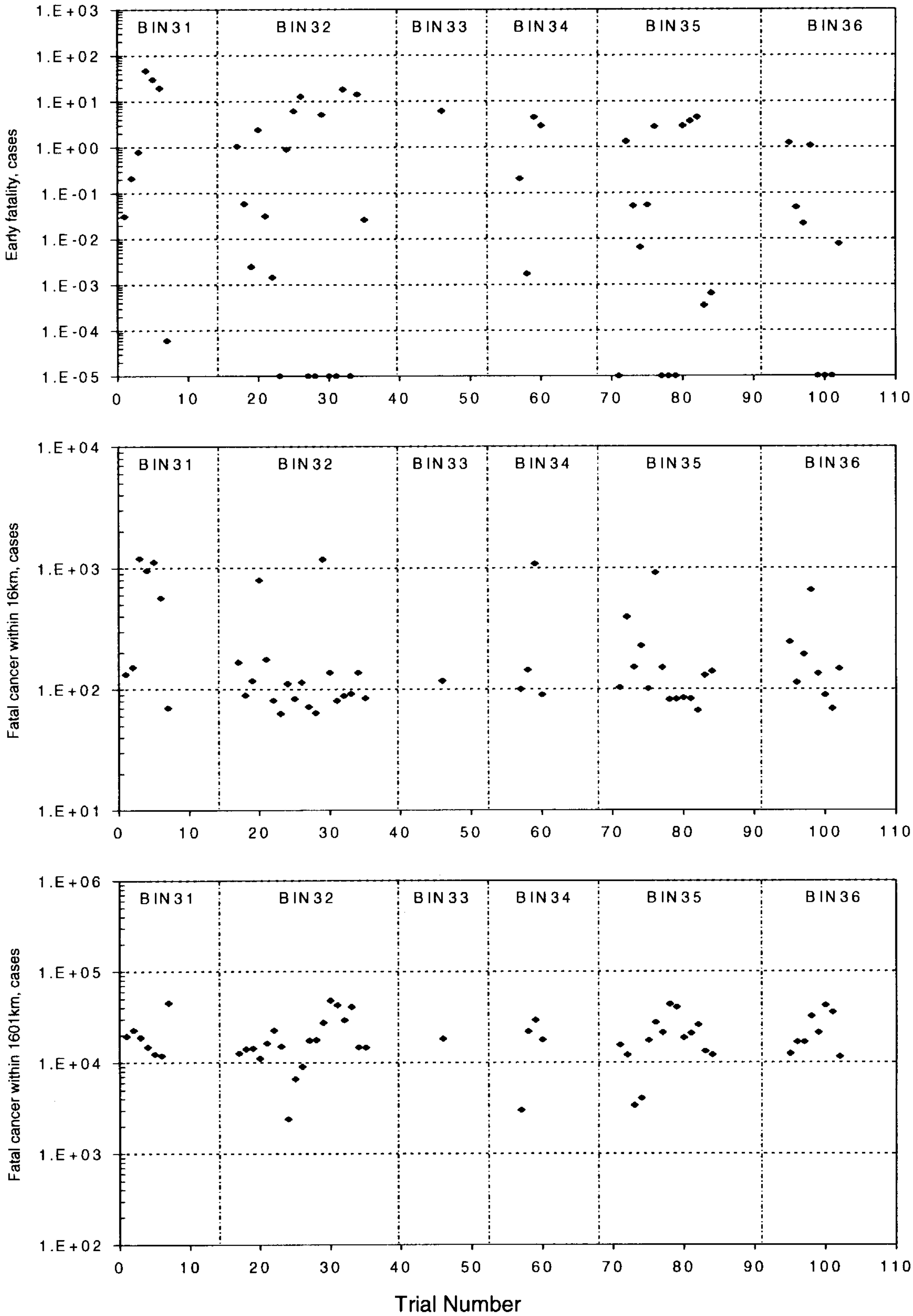

Figure 24. The variation of health effect estimation in BIN31, BIN32, BIN33, BIN34, BIN35 and BIN36. 7, 19, 1, 5, 14 and 5 weather sequences were completely sampled from BIN31 through BIN36, respectively.

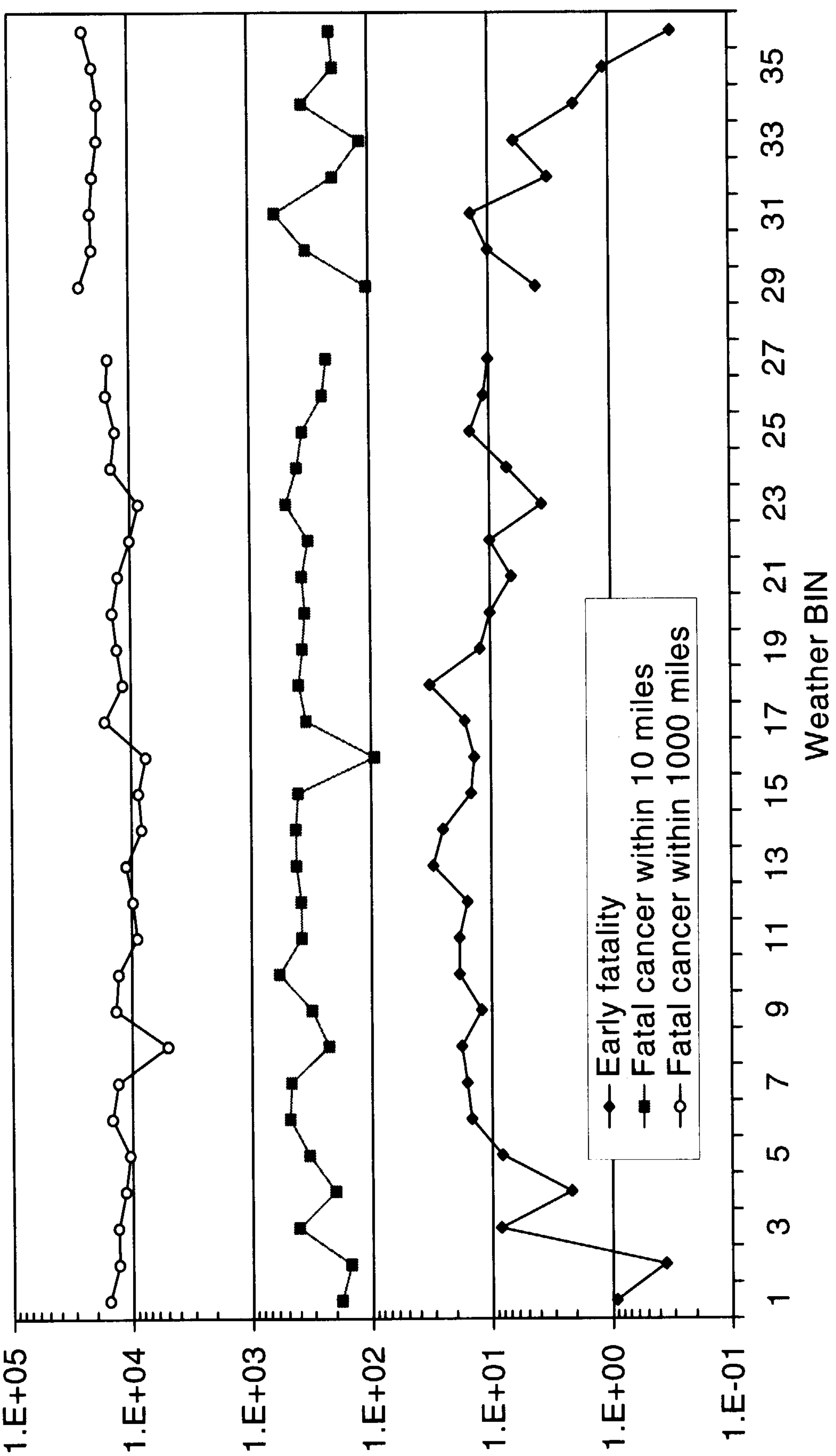

Figure 25. The average of health effect estimation results in each BIN, including early fatality, and fatal cancer within 16km and 1601km. No sample available for BIN28.

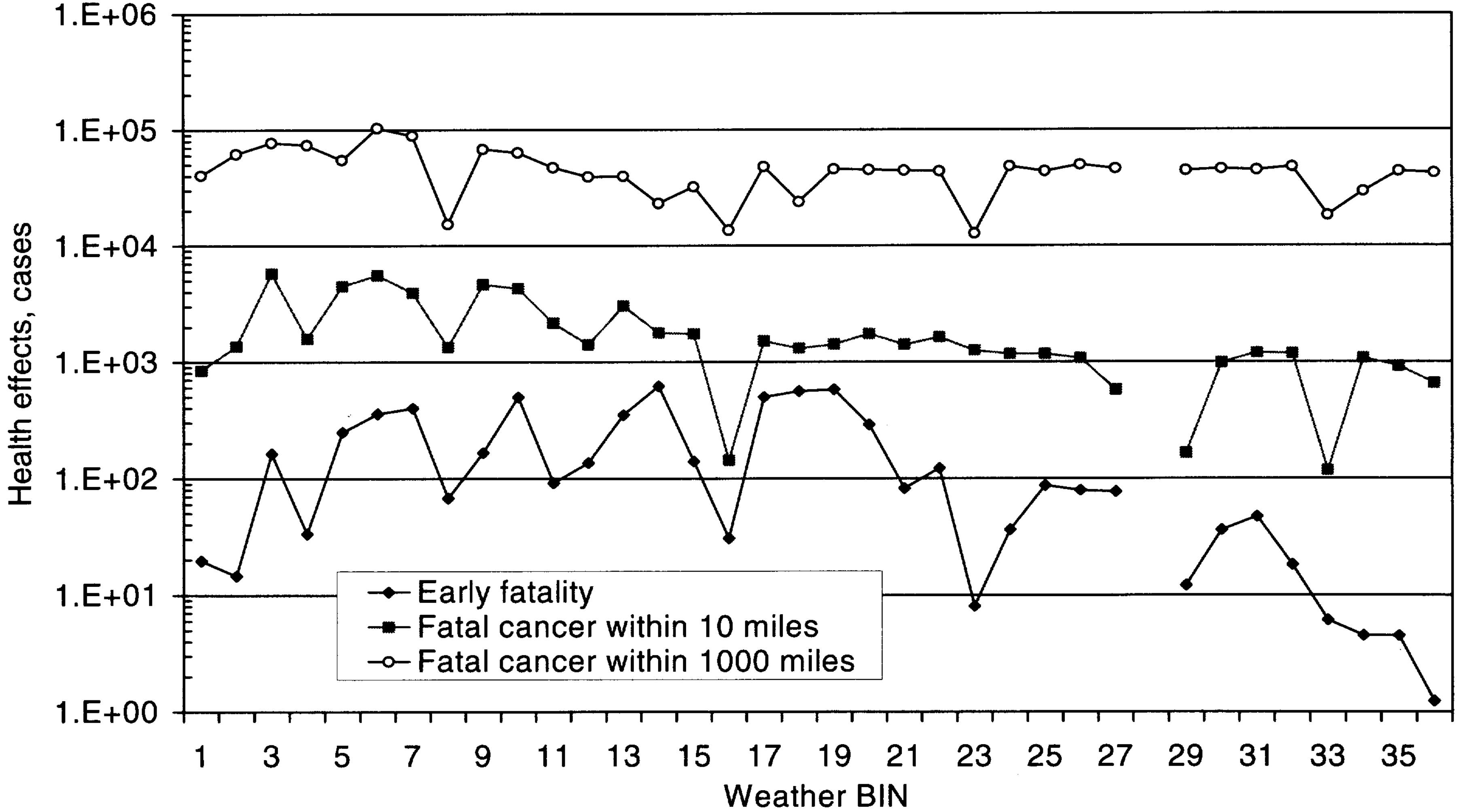

Figure 26. The maximum of health effect estimation results in each BIN, including early fatality, and fatal cancer within 16km and 1601km. No sample available for BIN28.

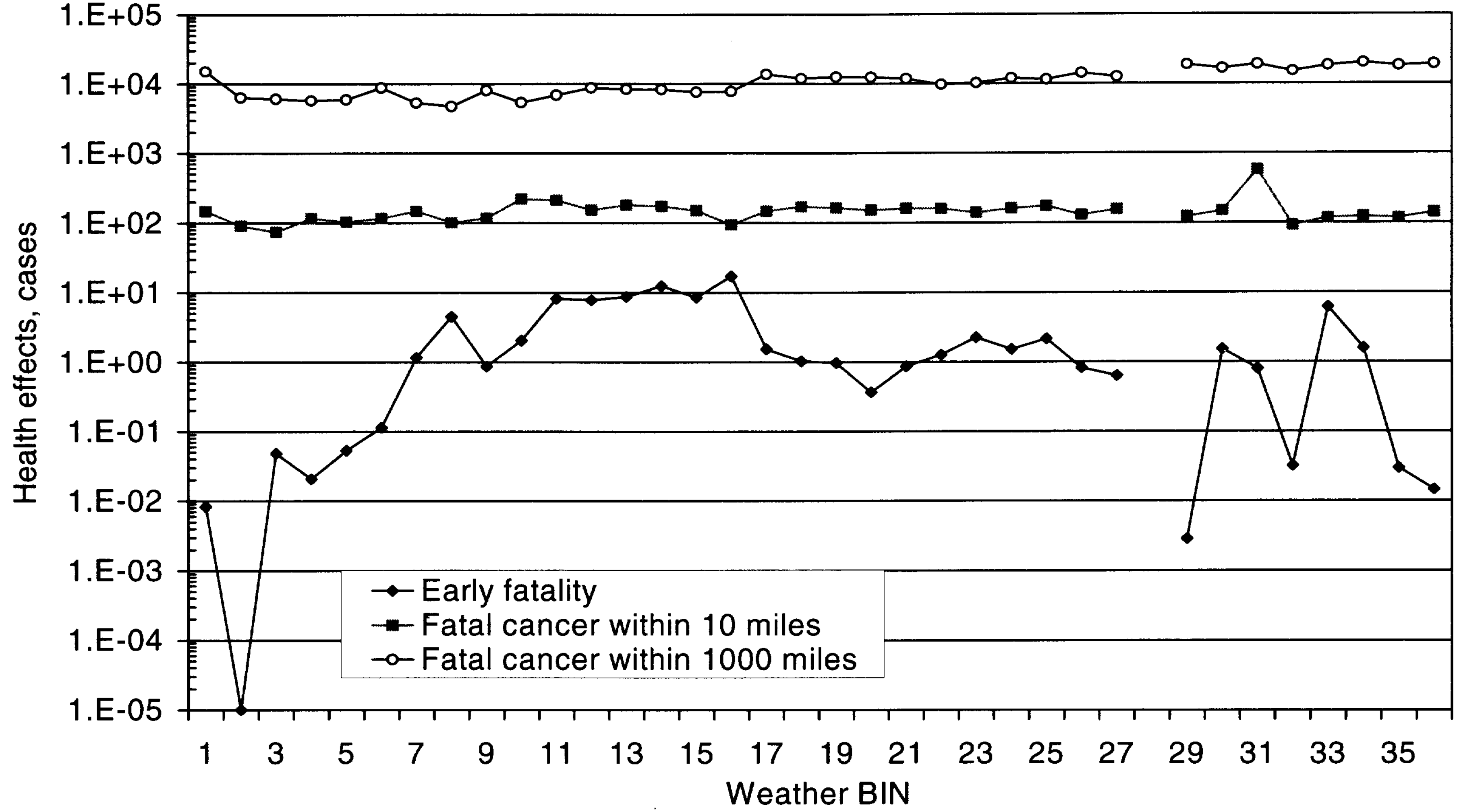

Figure 27. The median of health effect estimation results in each BIN, including early fatality, and fatal cancer within 16km and 1601km. No sample available for BIN28.

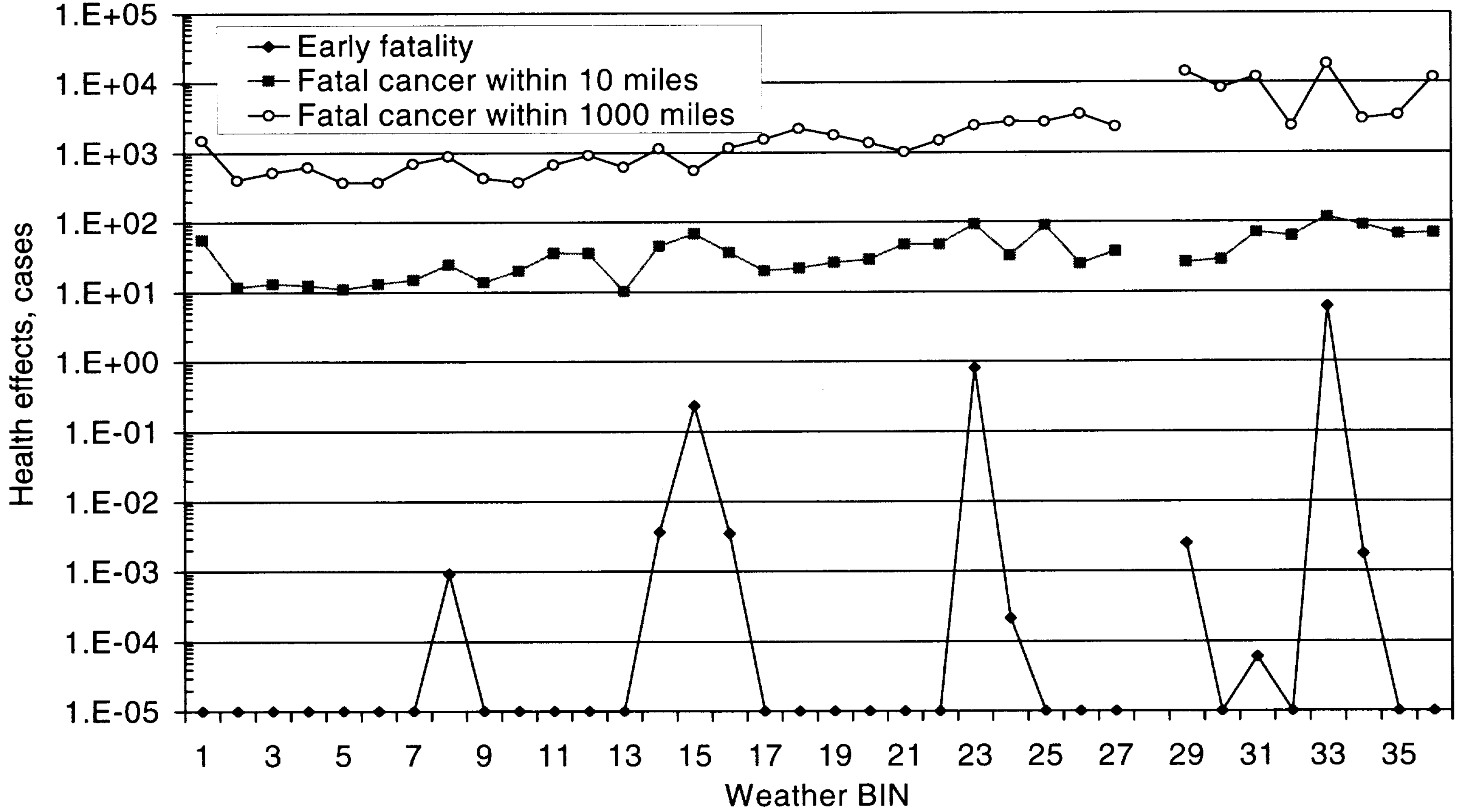

Figure 28. The minimum of health effect estimation results in each BIN, including early fatality, and fatal cancer within 16km and 1601km. No sample available for BIN28.

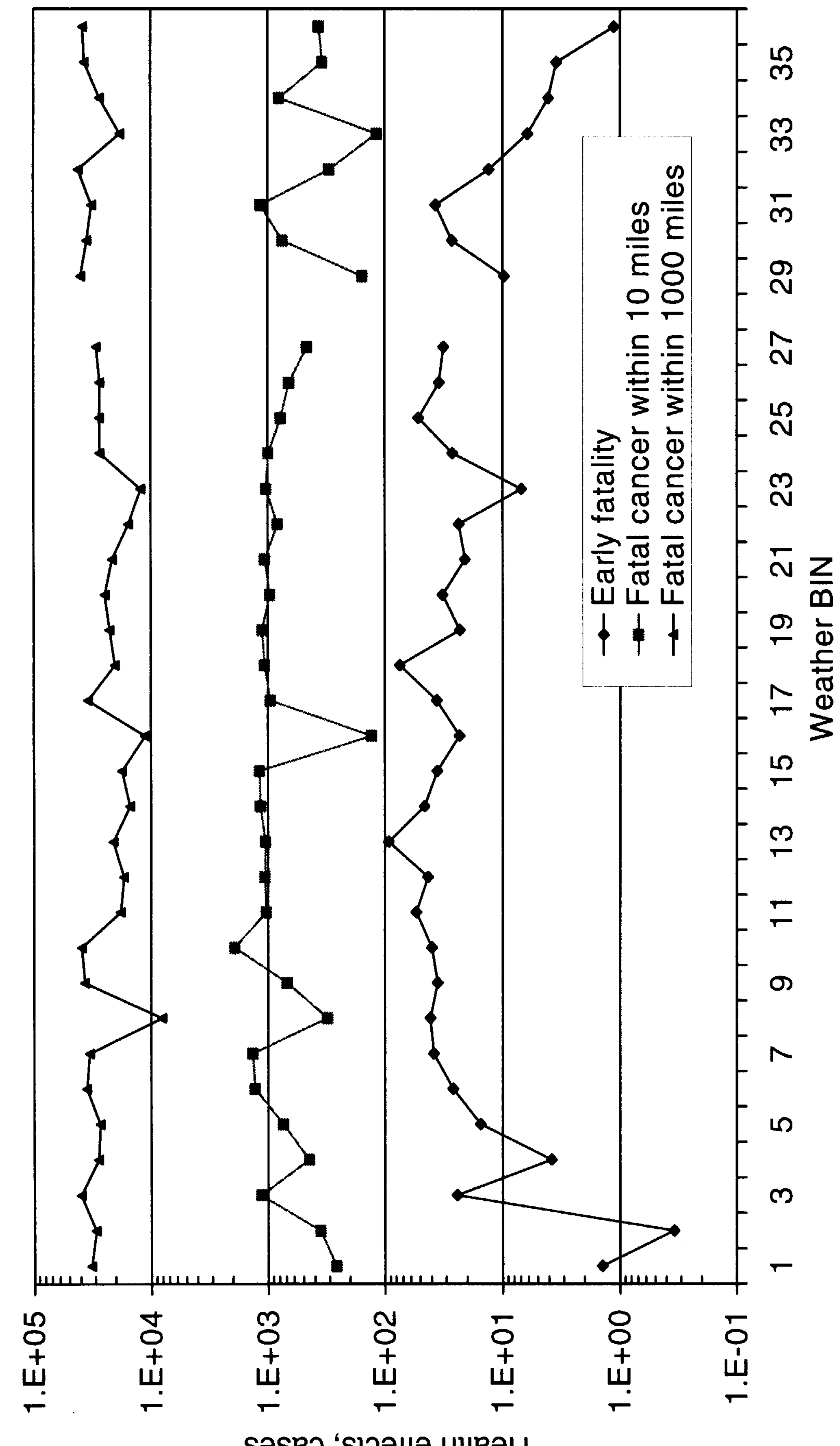

Figure 29. The 90 percentile values of health effect estimation results in each BIN, including early fatality, and fatal cancer within 16km and 1601 km. No sample available for BIN28.

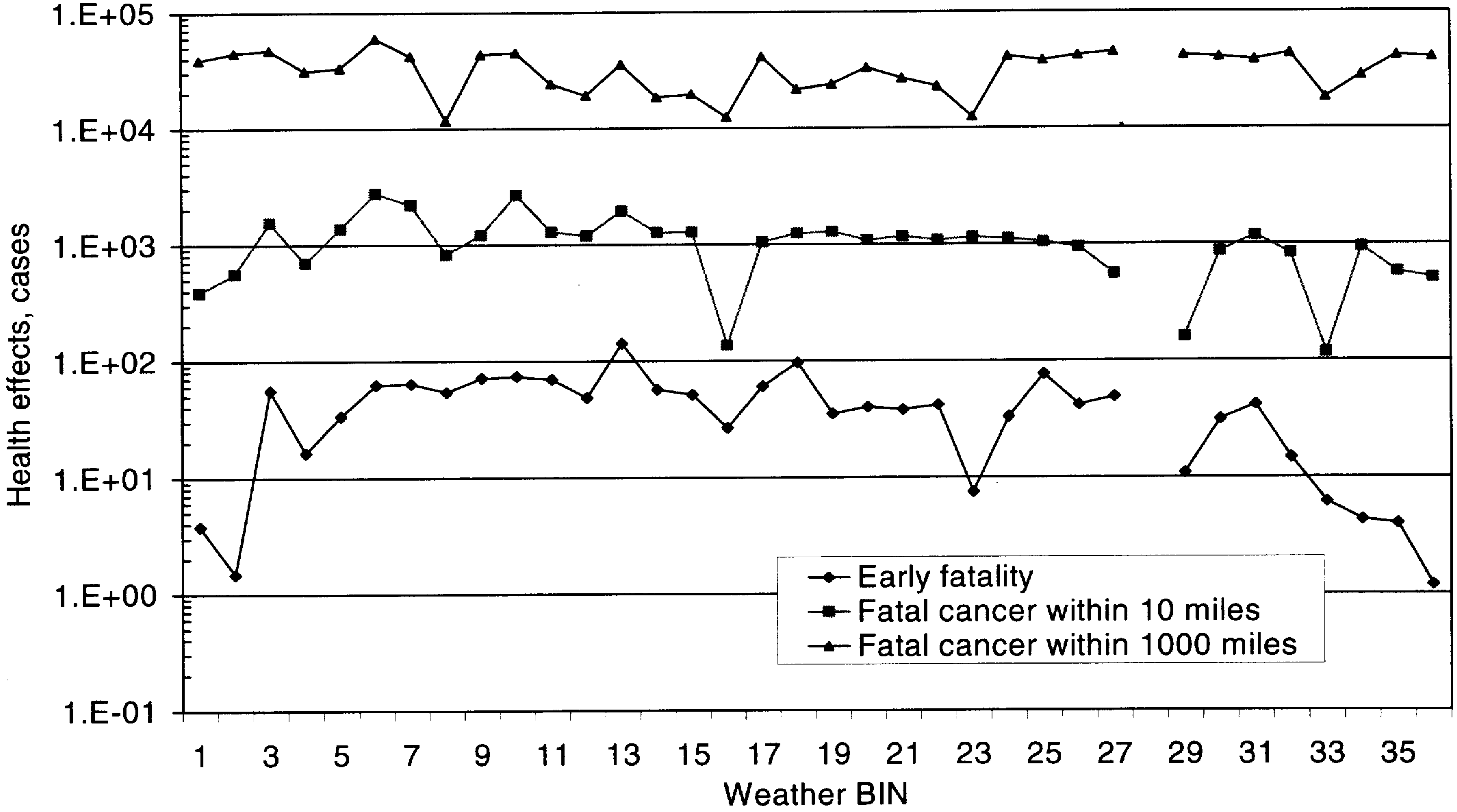

Figure 30. The 95 percentile values of health effect estimation results in each BIN, including early fatality, and fatal cancer within 16km and 1601 km. No sample available for BIN28.

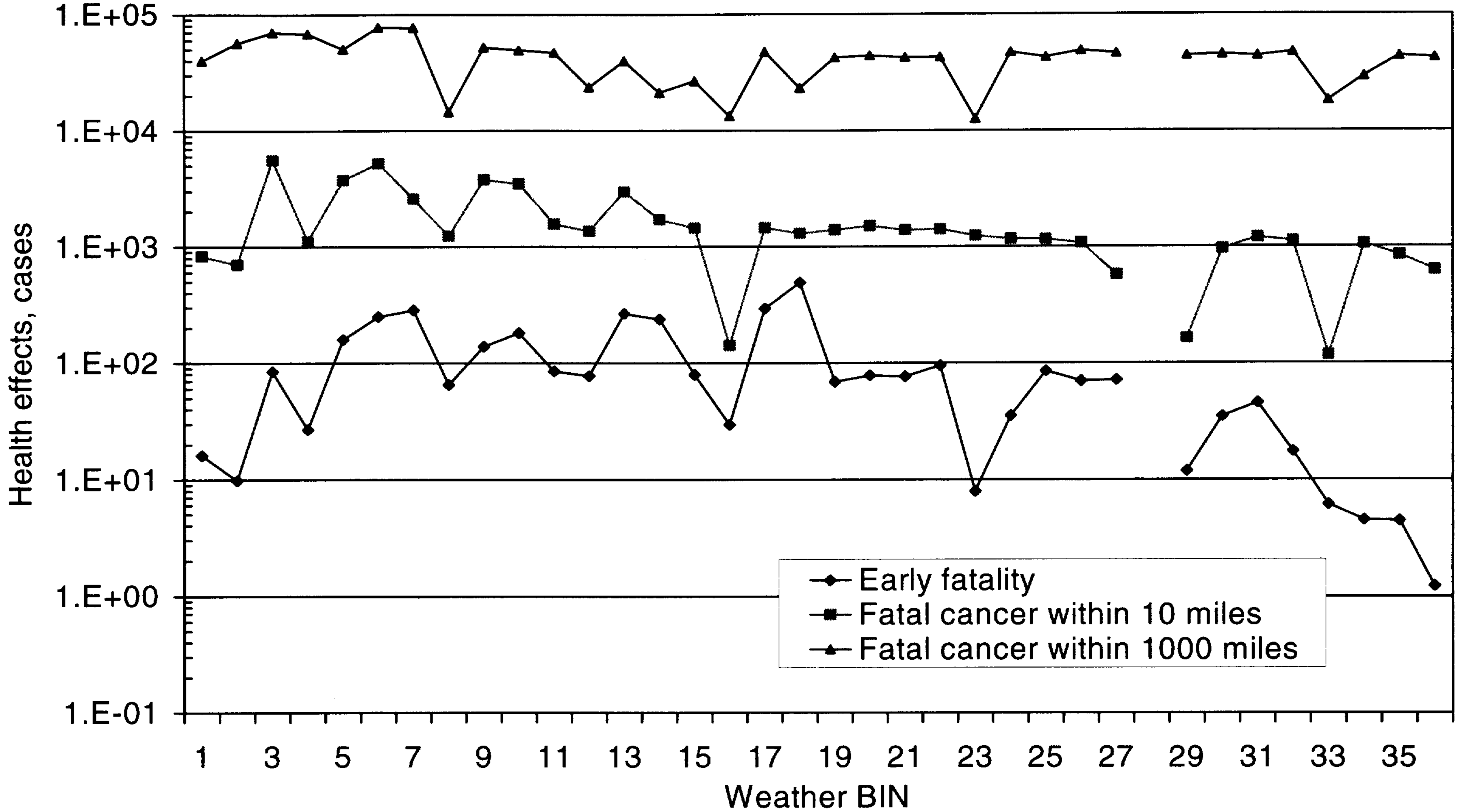

Figure 31. The 99 percentile values of health effect estimation results in each BIN, including early fatality, and fatal cancer within 16km and 1601 km. No sample available for BIN28.

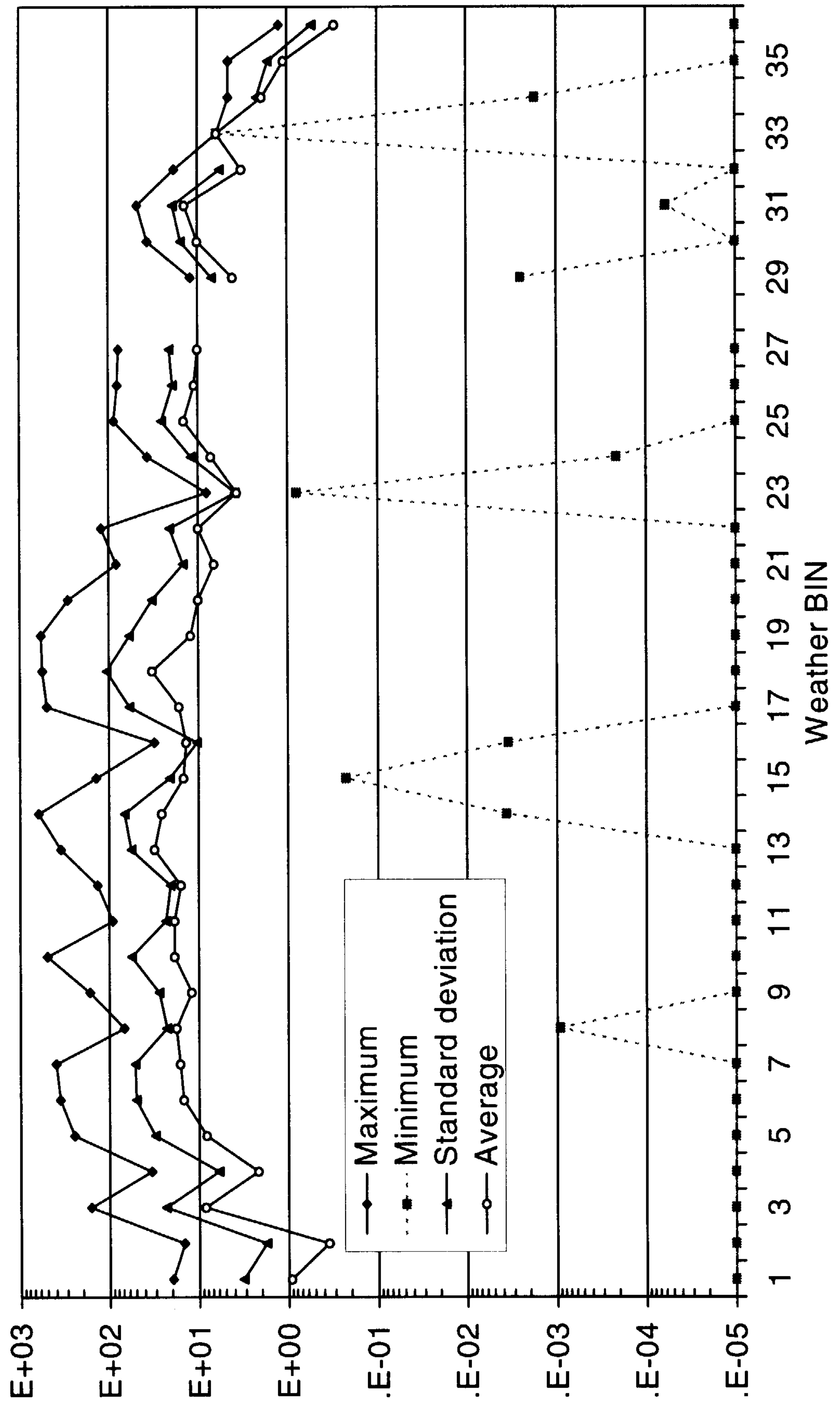

Figure 32. Comparison of some of statistical parameters of early fatality estimation results in each BIN, including the maximum, minimum, median and standard deviation. No sample available for BIN 28.

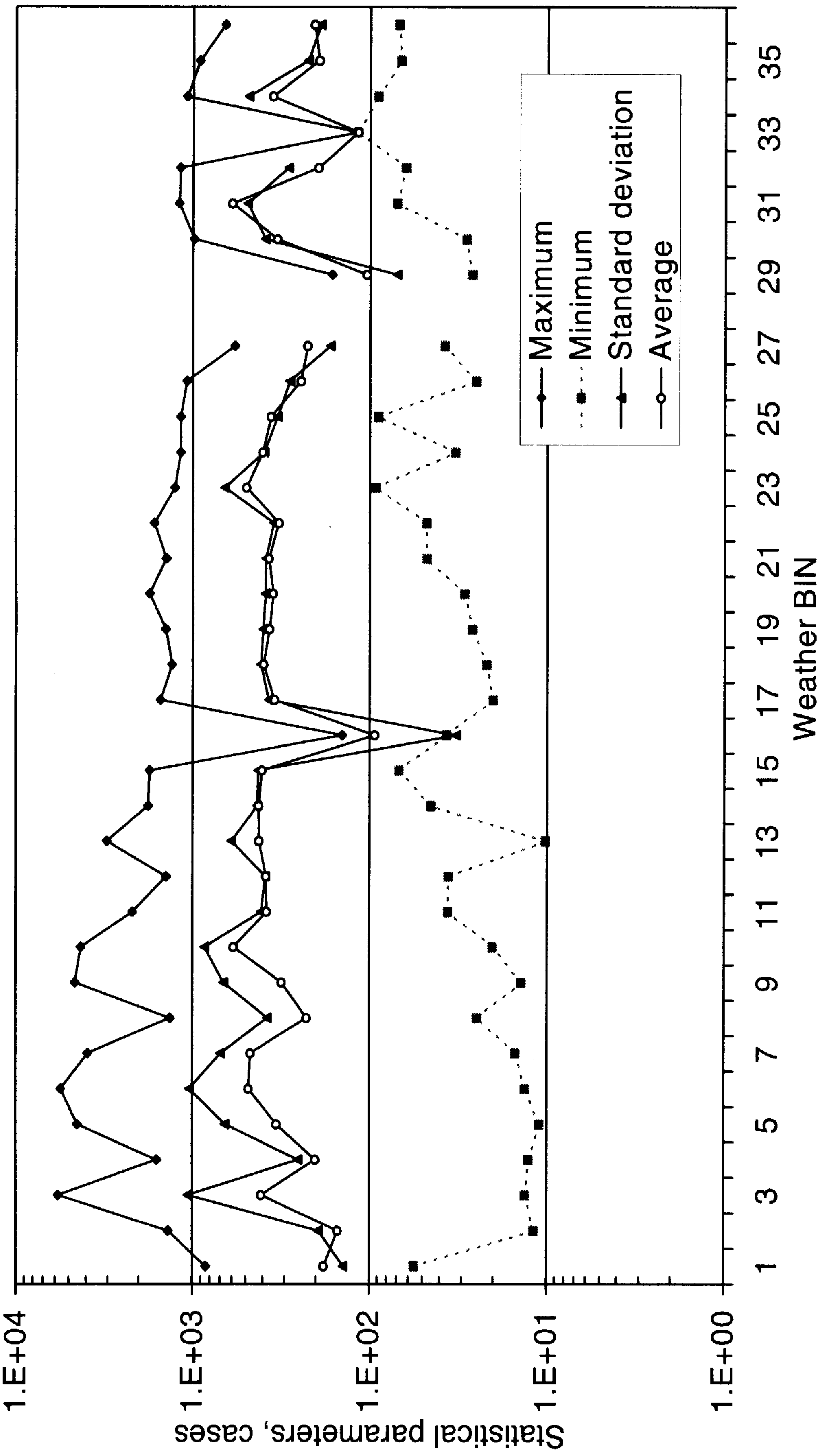

Figure 33. Comparison of some of statistical parameters of fatal cancer estimation results in each BIN within 16km, including the maximum, minimum, median and standard deviation. No sample available for BIN 28.

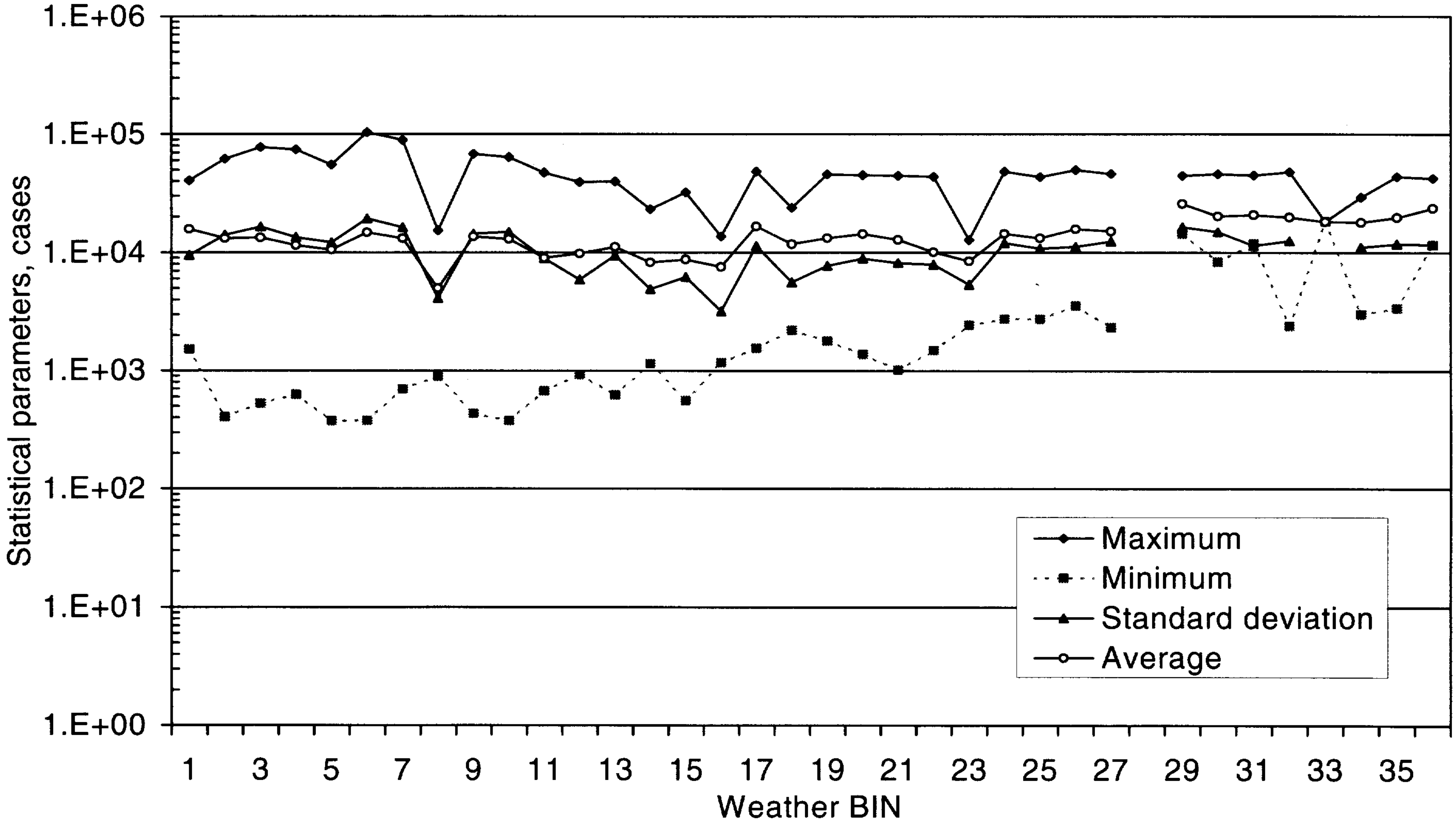

Figure 34. Comparison of some of statistical parameters of fatal cancer estimation results in each BIN within 1601km, including the maximum, minimum, median and standard deviation. No sample available for BIN 28.

This is a blank page.

国際単位系 (SI) と換算表

表 1　SI基本単位および補助単位

量	名　称	記　号
長さ	メートル	m
質量	キログラム	kg
時間	秒	s
電流	アンペア	A
熱力学温度	ケルビン	K
物質量	モル	mol
光度	カンデラ	cd
平面角	ラジアン	rad
立体角	ステラジアン	sr

表 2　SIと併用される単位

名　称	記　号
分，時，日	min, h, d
度，分，秒	°, ′, ″
リットル	l, L
トン	t
電子ボルト	eV
原子質量単位	u

$1\ eV = 1.60218 \times 10^{-19} J$

$1\ u = 1.66054 \times 10^{-27} kg$

表 5　SI接頭語

倍数	接頭語	記　号
10^{18}	エクサ	E
10^{15}	ペタ	P
10^{12}	テラ	T
10^{9}	ギガ	G
10^{6}	メガ	M
10^{3}	キロ	k
10^{2}	ヘクト	h
10^{1}	デカ	da
10^{-1}	デシ	d
10^{-2}	センチ	c
10^{-3}	ミリ	m
10^{-6}	マイクロ	μ
10^{-9}	ナノ	n
10^{-12}	ピコ	p
10^{-15}	フェムト	f
10^{-18}	アト	a

表 3　固有の名称をもつSI組立単位

量	名　称	記号	他のSI単位による表現
周波数	ヘルツ	Hz	s^{-1}
力	ニュートン	N	$m \cdot kg/s^2$
圧力，応力	パスカル	Pa	N/m^2
エネルギー，仕事，熱量	ジュール	J	N·m
工率，放射束	ワット	W	J/s
電気量，電荷	クーロン	C	A·s
電位，電圧，起電力	ボルト	V	W/A
静電容量	ファラド	F	C/V
電気抵抗	オーム	Ω	V/A
コンダクタンス	ジーメンス	S	A/V
磁束	ウェーバ	Wb	V·s
磁束密度	テスラ	T	Wb/m^2
インダクタンス	ヘンリー	H	Wb/A
セルシウス温度	セルシウス度	℃	
光束	ルーメン	lm	cd·sr
照度	ルクス	lx	lm/m^2
放射能	ベクレル	Bq	s^{-1}
吸収線量	グレイ	Gy	J/kg
線量当量	シーベルト	Sv	J/kg

表 4　SIと共に暫定的に維持される単位

名　称	記　号
オングストローム	Å
バーン	b
バール	bar
ガル	Gal
キュリー	Ci
レントゲン	R
ラド	rad
レム	rem

$1\ Å = 0.1\ nm = 10^{-10} m$

$1\ b = 100\ fm^2 = 10^{-28} m^2$

$1\ bar = 0.1\ MPa = 10^5 Pa$

$1\ Gal = 1\ cm/s^2 = 10^{-2} m/s^2$

$1\ Ci = 3.7 \times 10^{10} Bq$

$1\ R = 2.58 \times 10^{-4} C/kg$

$1\ rad = 1\ cGy = 10^{-2} Gy$

$1\ rem = 1\ cSv = 10^{-2} Sv$

（注）

1. 表1－5は「国際単位系」第5版，国際度量衡局 1985年刊行による。ただし，1 eV および 1 u の値は CODATA の1986年推奨値によった。
2. 表4には海里，ノット，アール，ヘクタールも含まれているが日常の単位なのでここでは省略した。
3. bar は，JISでは流体の圧力を表わす場合に限り表2のカテゴリーに分類されている。
4. EC閣僚理事会指令では bar，barn および「血圧の単位」mmHg を表2のカテゴリーに入れている。

換　算　表

力	$N (=10^5 dyn)$	kgf	lbf
	1	0.101972	0.224809
	9.80665	1	2.20462
	4.44822	0.453592	1

粘　度　$1\ Pa \cdot s (N \cdot s/m^2) = 10\ P$(ポアズ)$(g/(cm \cdot s))$

動粘度　$1\ m^2/s = 10^4 St$(ストークス)(cm^2/s)

圧力	MPa(=10 bar)	kgf/cm^2	atm	mmHg(Torr)	lbf/in^2(psi)
	1	10.1972	9.86923	7.50062×10^3	145.038
	0.0980665	1	0.967841	735.559	14.2233
	0.101325	1.03323	1	760	14.6959
	1.33322×10^{-4}	1.35951×10^{-3}	1.31579×10^{-3}	1	1.93368×10^{-2}
	6.89476×10^{-3}	7.03070×10^{-2}	6.80460×10^{-2}	51.7149	1

エネルギー・仕事・熱量	$J (=10^7 erg)$	kgf·m	kW·h	cal(計量法)	Btu	ft·lbf	eV
	1	0.101972	2.77778×10^{-7}	0.238889	9.47813×10^{-4}	0.737562	6.24150×10^{18}
	9.80665	1	2.72407×10^{-6}	2.34270	9.29487×10^{-3}	7.23301	6.12082×10^{19}
	3.6×10^6	3.67098×10^5	1	8.59999×10^5	3412.13	2.65522×10^6	2.24694×10^{25}
	4.18605	0.426858	1.16279×10^{-6}	1	3.96759×10^{-3}	3.08747	2.61272×10^{19}
	1055.06	107.586	2.93072×10^{-4}	252.042	1	778.172	6.58515×10^{21}
	1.35582	0.138255	3.76616×10^{-7}	0.323890	1.28506×10^{-3}	1	8.46233×10^{18}
	1.60218×10^{-19}	1.63377×10^{-20}	4.45050×10^{-26}	3.82743×10^{-20}	1.51857×10^{-22}	1.18171×10^{-19}	1

1 cal = 4.18605 J（計量法）
　= 4.184 J　（熱化学）
　= 4.1855 J　（15 °C）
　= 4.1868 J（国際蒸気表）

仕事率　1 PS（仏馬力）
　= 75 kgf·m/s
　= 735.499 W

放射能	Bq	Ci
	1	2.70270×10^{-11}
	3.7×10^{10}	1

吸収線量	Gy	rad
	1	100
	0.01	1

照射線量	C/kg	R
	1	3876
	2.58×10^{-4}	1

線量当量	Sv	rem
	1	100
	0.01	1

（86年12月26日現在）

Variation of Radiological Consequences under Various Weather Conditions